МІНІСТЕРСТВО ОСВІТИ І НАУКИ УКРАЇНИ

НАЦІОНАЛЬНИЙ АВІАЦІЙНИЙ УНІВЕРСИТЕТ

Факультет літальних апаратів
Кафедра авіаційних двигунів

ДОПУСТИТИ ДО ЗАХИСТУ
Завідувач кафедри
Докт.техн. наук , проф.
_____Терещенко Ю.М.
"____" _____2022 р.

Тема: *Удосконалення опор роторів двоконтурних турбореактивних двигунів, що_____ використовуються в силових установках дальньомагістральних літаків*

Виконавець: _____Лю Чуаньфу

Керівник: к.т.н., проф. _____Гвоздецький І. І.

Консультанти з розділів:

охорона праці: к.т.н., _____ _Кажан К. І._____

охорона навколишнього
середовища: к.т.н. , доцент _____Павлюх Л.І.

Нормоконтролер :_____ /_____/

КИЇВ 2022

MINISTRY OF EDUCATION AND SCIENCE OF UKRAINE

NATIONAL AVIATION UNIVERSITY

Aircraft Faculty
Aeroengines Department

PERMISSION TO DEFEND

Head of department
Doctor of science, professor
_____ Yu. Tereshchenko
"____" _____2022

MASTER'S DEGREE THESIS

Topic: *Methods to Improve the Rotor Supports of Turbofan Engines for Long-range Passenger Airplanes.*

Fulfilled by: Liu chuan fu

Supervisor:

Candidate of science (Engineering), assoc.prof. _____ Gvozdetskyi I.I.

Labour precautions advisor:
Candidate of science (Engineering), assoc.prof _____ Kazhan K. I.

Environmental protection advisor:
Candidate of science (Engineering), assoc.prof. _____ Pavliukh L. I.

Standards Inspector _____/_____/

Kyiv 2022

NATIONAL AVIATION UNIVERSITY

Faculty: The Aerospace faculty

Department: The Aeroengines Department

Educational and Qualifications level: Master's Degree

The specialty: 272 Technical Maintenance of Aircraft and Aeroengines

APPROVED BY

Head of the Department

_____ Yu. Tereshchenko

" " 20 22

Graduate Student's Degree Thesis Assignment

Name: Лю Чуаньфу (in English)

1. The Thesis Topic: *(Methods to Improve the Rotor Supports of Turbofan Engines for Long-range_ Passenger Airplanes)*

approved by the Rector's order of " 9 " 10 2022 № ????/cm

2. The Graduation Project to be performed from : 01. *10. 2022* to *24. 11. 2022*

3. Initial data for the thesis : Perform calculations for gas turbine engine standard conditions (V=0; H=0; IST), to improve the reliability and service life of the GTE bearings, patent analysis on developed problem.

4. The content of the explanatory note: Introduction, analyses of today state and possible methods for improving turbofan engine effectiveness and reliability by improvement of it`s rotor supports due to usage of Ceramic Hybrid Bearings. Selection of main parameters of operation process and thermo –gas dynamic calculation

of turbofan engine and development of its constractive scheme*; General conclusion*

5. The list of mandatory graphic materials: Structural loaded diagram of projected engine; turbine unit drawing; principle diagrams of engine systems; graphic materials for innovation part of the diploma work.

6. Time and Work Schedule

7. Advisers on individual sections of the work (Thesis):

		Date, Signature

order #	**Stages of Graduation Project Completion**	**Stage Completion Dates**	**Remarks**
1	Review of the literature on the problem being developed and the choice of a method for solving the problem	01.10.2022 05.10.2022	Done
2	Review of patents on the problem under development	06.10.2022~ 08.10.2022	Done
3	Selection of operation parameters for the designed engine	09.10.2022 16.10.2022	Done
4	Thermodynamic and gas dynamic calculation	17.10.2022 20.10.2022	Done
5	Development of the structural and power scheme of the engine	21.10.2022 24.10.2022	Done
6	Special part: Design development and calculation of Ceramic Hybrid Bearings	25.10.2022 30.10.2022	Done
7	Development of the engine oil system and analysis of the effectiveness of the proposed measures for the application of Ceramic Hybrid Bearings	01.11. 2022 14.11.2022	Done
8	Labor precaution	15.11.2022 16.11.2022	Done
9	Ecology protection	16.11.2022 18.11.2022	Done
10	Arrangement of graphic materials (structural scheme of the engine and diagram of the oil system of the engine). Arrangement of explanatory note	18.11.2022 20.11.2022	Done

Section Adviser

		Assignment Delivered	Assignment Accepted
Labour precaution	Kazhan K. I.		
Ecology	Pavliukh L. I.		

8. Assignment issue date: 29 . 09 . 2022

Graduate Project Supervisor: Gvozdetskyi I.I. _____
(supervisor signature)

Assignment is accepted for performing:

Graduate student: Лю Чуаньфу Лю Чуаньфу
2022.10.9 _____

ABSTRACT

The explanatory note to the diploma work “Methods to Improve the Rotor Supports of Turbofan Engines for Long-range_ Passenger Airplanes”

`

Key words

strength, Ceramic Hybrid Bearings, Turbofan Engines,

improving effectiveness, design shaft and bearing, design engine,

The research object – the evaluation of design, and reliability and structural integrity of Rotor Supports of Turbofan Engines for Long-range_ Passenger Airplanes.

The research subject – the development of recommendations directed at improving the workability and maintainability of Rotor Supports by improvement of rotor supports due to usage of Ceramic Hybrid Bearings.

The purpose of diploma work – the development of recommendations, directed on improvement of improving turbofan engine effectiveness and reliability by improvement of rotor supports due to usage of Ceramic Hybrid Bearings.

Method of research –Selection of operation parameters for the designed engine, Development of the structural and power scheme of the engine, Development of the engine oil system and analysis of the effectiveness of the proposed measures for the application of Ceramic Hybrid Bearings

The optimal essence of this diploma work is to ensure Turbofan engine effectiveness for Long-range_ Passenger Airplanes improving the workability and maintainability of Rotor Supports by improvement of rotor supports due to usage of Ceramic Hybrid Bearings.

Diploma work materials are recommended to use in educational process and practical activity of specialists of development laboratory.

(graduate student’s signature) (Date)

CONTENTS

Introduction

Projected engine is based on the engine GEnx prototype, The General Electric GEnx ("General Electric Next-generation") is an advanced dual rotor, axial flow, high-bypass turbofan jet engine in production by GE Aviation for the Boeing 787 and 747-8.The double -circuit turbojet engine (TRDD) has a design that allows to move additional masses of air that passes through the outer circuit of the engine. This design provides the higher efficiency than the usual TRD. The first concept of TRDD in aircraft engineering was proposed by the Ukrainian designer of the aircraft engines Архип Люлька . On the basis of the experiments conducted since 1937, Архип Люлька applied for the invention of two -circuit TRD .

But critical assessment of the situation reveals that The main advantage of this engine is their high efficiency. Disadvantages -Large weight and size. Especially the large diameter of the fan, which leads to a significant air resistance in the flight. The scope of such engines is a mid -length commercial airliner and military transportation aviation. So engine necessitates changes in order to improve previously mentioned qualities such as: thrust, efficiency, fuel consumption, durability, weight, and size.

One of their methods is to improve the rotor Supports to reduce resistance of the dual -circuit turbine engine with the help of Ceramic Hybrid Bearings

The aim of diploma work is comprised in defining and identifying of the problems which cause negative influences on the engine and to propose methods of their either decrease or elimination with the help of Ceramic Hybrid Bearings as bearing assemblies.

Ceramic Hybrid Bearings (CHB) : they combine steel rings and ceramic rolling elements, whereas more conventional bearings use steel for both. The silicon-nitride of the ceramic rollers is “bearing grade” — the highest quality available. Ceramic Balls are suitable for applications where high loads, high speeds and extreme temperatures are factors. Long life and the need for minimal lubrication make this material appropriate for extreme applications. Ceramic is non-porous, non-magnetic, non corrosive and lighter than steel. In ball form, ceramic balls are also harder than steel and because ceramic balls are non-porous they are virtually frictionless and capable of spinning faster than steel balls[1].

This innovation gives an opportunity to:

- Application of high load, high speed and extreme temperature
- Ceramics, magnetic, non -corrosive and lighter than steel

- ,Reduce engine weight; Increase endurance;
- need less lubrication and have higher hardness,
- They have almost no friction and can rotate faster than steel balls
- Multi-purpose use in variety of machines and production lines
- Increase fault tolerance; extend the life of the bearing
- High efficiency, low weight and small size

Ceramic hybrid ball bearings, especially silicon nitride, mixed ceramic bearing, have the characteristics of low density, high hardness, low friction coefficient, anti -magnetic electrical insulation, abrasion resistance, self -lubrication, and good rigidity. High temperature resistance, high wear resistance, high speed -speed convection, friction and heat calories are greatly reduced, long service life is 3 to 5 times the full steel bearings, weight light ceramic materials are 60%lighter than steel, and the same rigidity than steel, and the same rigidity.[2] The elastic mold of ceramic materials is 50%higher than the bearing steel. In ball form, ceramic balls are also harder than steel and because ceramic balls are non-porous they are virtually frictionless and capable of spinning faster than steel balls. Because ceramic is a glass like surface it has an extremely low coefficient of friction and is ideal for applications seeking to reduce friction. Ceramic balls require less lubrication and have a greater hardness than steel balls which will contribute to increased bearing life. Thermal properties are better than steel balls resulting in less heat. Ceramic hybrid bearings are widely used in electric motors, aerospace applications, performance racing vehicles, laboratory equipment, under water applications and more. Any application that requires higher speeds, lower friction and longer life are ideal for ceramic hybrid bearings.[3]

CHAPTER 1. ANALYSIS OF CERAMIC HYBRID BEARINGS

1.1 The problem of affecting aircraft engine rotor

The fault types of aero-engine are very complex, which can be divided into performance fault, structural strength fault and accessory system fault. From the fault statistics of aero-engine, it is found that engine performance faults account for about 10 % ~ 20 % of the total faults, and structural strength faults account for about 60 % ~ 70 % of the total faults. In either case, the precursor and development of the fault is reflected in the vibration of the engine rotor.

Rotor system is the core system of aero-engine. Once a fault occurs, it will affect the work and cause serious destructive accidents. Therefore, it is an important task to study the vibration phenomenon and mechanism of aero-engine rotor system caused by various factors. The research can not only provide a theoretical basis for effective fault diagnosis and control, but also provide a dynamic theoretical basis for solving the key mechanical problems in advanced aero-engine design.

In the high-speed rotating compressor and turbine system of aero-engine, rolling bearing is still a component prone to failure. Field studies show that about 90 % of rolling bearing failures are related to defects in the inner or outer ring, and the other 10 % are related to faults in the rolling element or cage. In addition, there are strong nonlinear factors in rolling bearings. In order to solve the fault of rolling bearings, the nonlinear dynamic mechanism should be studied in depth.

The aero-engine rotor system has many fault modes and complex mechanisms. More importantly, each fault often does not exist alone. One fault usually causes or is accompanied by other faults. The coupling of multiple faults and the existence of nonlinear factors greatly increase the difficulty of dynamic analysis, which brings great challenges and opportunities to our research work.

Conclusion: in order to solve the problem ,the development of recommendations, directed on improvement of improving turbofan engine effectiveness and reliability by improvement of rotor supports due to usage of Ceramic Hybrid Bearings.

1.2 The essence of the solution

MRC hybrid bearings lower the risk of failure in the generator and increase

reliability. The bearing design, which combines a ceramic (silicon nitride) rolling element with conventional steel rings, eliminates the risk of electrical damage and the huge repair costs and lost energy production associated with it.

MRC hybrid bearing benefits include: • Superior electrical insulation properties even against very high frequency currents • Extended maintenance intervals due to longer grease life • Reliable operation even under poor lubrication and contaminated environment • Greater wear resistance against solid particles • Easy upgrade of already installed turbines • Extended service life • Reduced life cycle cost and total cost of operation

Modern aircraft require more on-board electrical power than ever before. Increasing the size of starter/generators to provide these additional requirements inevitably increases their mass. Instead, starter/generators manufacturers are considering increasing their operational speed. The rotational speeds of the newer generation of starter/generators are expected to approach 30,000 rpm. This will impose severe loading demands on the currently employed bearings; which can lead to earlier degradation due to harsher rolling contact fatigue (RCF). Additionally, bearings in starter/generators experience severe operational conditions, e.g., extreme temperature, vibration and electrical interference. In response to these new requirements, bearing designers are turning to hybrid bearings for the newest generation of starter/generators. However, not much is known about hybrid bearings wear behavior in this application.

The gas turbine engine generally includes an inlet section, a compressor section, a combustion section, and a turbine section in a serial order section and exhaust section. In operation, air enters the inlet section and flows to the compressor section, in the compressor section, one or more An axial compressor gradually compresses the air until the air reaches the combustion zone. The fuel is mixed with compressed air and is burning Combustion in the section, resulting in combustion gas. Burning gas flows from the combustion section through the hot gas path confined to the turbine section and then leaving the turbine section through the exhaust section. In specific configurations, the compressor sections include low pressure compressors (LPCs) and high pressure compressors in serial order (HPC). LPC and HPC can include one or more axially separated stages. Each level may include a row of circumferentially spaced The stator stator blades and a row of circumferentially spaced rotor blades located downstream of the stator blades. Stator stator blade will flow over pressure

The air in the shrink section is guided to the rotor blade, and the rotor blade transfers the kinetic energy to the air to increase its pressure. Pressurized air leaving the HPC can then flow into the burner where fuel is injected into the pressurized air flow The obtained mixture is burned in the burner. High energy combustion products are induced from the combustion chamber along the hot gas path of the engine High pressure turbine (HPT) for HPC driven by high pressure drive shaft and then to low pressure turbine for LPC (LPT). After driving each of LPT and HPT.

1.3 Solution of the problem

Hybrid bearings are typically constructed using rolling elements made of a ceramic material such as silicon nitride, running over fatigue resistant steel raceways. Critically, ceramic materials' mass can be up to 60 % lower than that of conventional ball bearings, resulting in lower centrifugal loading and skidding [1]. Some of the most

recognized performance benefits of hybrid bearings include [2]: higher rotational speed, longer life, lower heat generation and superior starvation tolerance.

Hybrid bearings are typically constructed using rolling elements made of a ceramic material such as silicon nitride, running over fatigue resistant steel raceways. Critically, ceramic materials' mass can be up to 60 % lower than that of conventional ball bearings, resulting in lower centrifugal loading and skidding [1]. Some of the most recognized performance benefits of hybrid bearings include [2]: higher rotational speed, longer life, lower heat generation and superior starvation tolerance.

Principles of rotor support operation

Referring now to the accompanying figure, Figure 1 shows a cross-sectional view of an embodiment of a gas turbine engine 10 that can be used in an aircraft in terms of this subject. For reference purposes, engine 10 is shown to have a longitudinal or axial central axis 12 extending through it. Typically, engine 10 may include a core gas turbine engine (usually indicated by the accompanying diagram marker 14) and a fan section 16 positioned upstream of it. The core engine 14 can usually include a basically tubular outer shell 18 with a defined annular inlet 20. In addition, the outer housing 18 further seals and supports the low-pressure booster compressor 22, which is used to feed the The pressure of the air entering the core engine 14 is increased to the first pressure level. The high-pressure multistage axial compressor 24 can then receive pressurized air from the booster compressor 22 and further increase the pressure of this air. The pressurized air leaving the high-pressure compressor 24 can then flow to the burner 26. The fuel is injected into the pressurized air flow in the burner 26, and the resulting mixture burns in the burner 26. High energy combustion products are directed from combustion chamber 26 along the hot gas path of engine 10 to the first (high pressure) turbine 28 used to drive the high pressure compressor 24 via the first (high pressure) drive shaft 30, and then to the second (low pressure) turbine 28 used to drive the high pressure compressor 24 via the second (low pressure) drive shaft 30. The second (low pressure) turbine 32 of the booster compressor 22 and the fan section 16 is driven by the second (low pressure) drive shaft 34. The second drive shaft is usually coaxial with the first drive shaft 30. After driving each of the turbines 28 and 32, the combustion product can be removed from the core via the exhaust nozzle 36 Engine 14 is discharged to provide propulsion jet thrust.

In addition, as shown in Figure 1, the fan section 16 of engine 10 can usually include a rotatable axial fan rotor assembly 38, which is constructed to be surrounded by an annular fan shell 40. General technicians in this field should understand that the fan housing 40 can be constructed from a plurality of basically radially extended, circumferentially spaced outlet-guided stator blades 42 relative to the core engine 14 Brace. Thus, the fan housing 40 can close the fan rotor assembly 38 and its corresponding fan rotor blades 44. In addition, the downstream section 46 of the fan housing 40 can be extended on the outer part of the core engine 14 to limit the secondary or bypass air duct 48 that provides additional propulsive jet thrust. It should be understood that in several embodiments, the second (low pressure) drive shaft 34 can be connected directly to the fan rotor assembly 38 to provide a direct drive configuration. Alternatively, the second drive shaft 34 may be connected to the fan rotor assembly 38 via gear reducer 37 (e.g. reduction gear or gearbox) to provide an

indirect drive or gear drive configuration. Such (one or more) reduction gear can also be set between any other suitable shaft and / or shaft in the engine as required or required. During the operation of engine 10. Initial air flow (indicated by arrow 50) is available through the fan housing. 40 of the associated inlet 52 enters the engine 10. Air flow 50 then passes through the fan blade 44 and splits into moving ducts. The pressure of the second compressed air flow 56 then increases and enters the high pressure compressor 24 (indicated by arrow 58). Mixing with fuel. After merging in the burner 26, the combustion product 60 leaves the burner 26 and flows through the

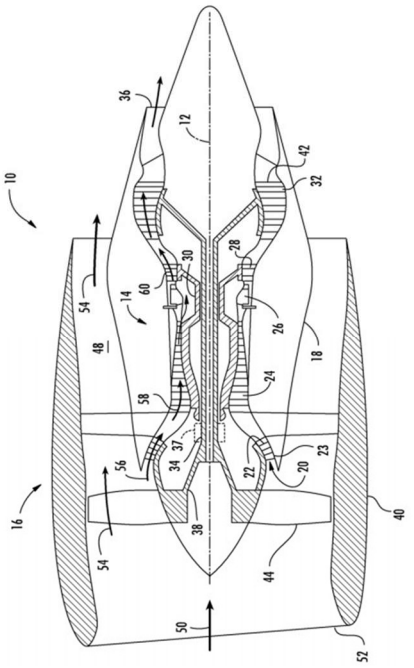

first turbine 28.

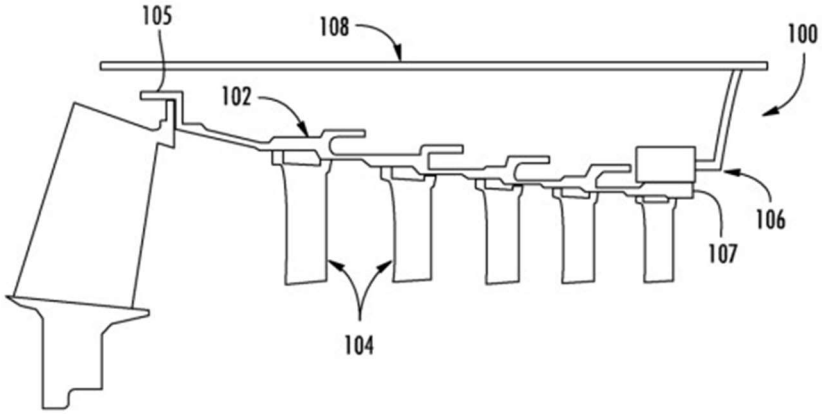

Thereafter, combustion products 60 flows through the second turbine 32 and leaves the exhaust nozzle 36 to provide thrust for engine 10. Referring now to Figure 2, rotations suitable for use in gas-turbine engine 10 are shown according to various aspects of this topic. A cross-sectional view of an embodiment of the sub-support system 100, showing in particular the high pressure relative to the gas turbine engine 10 Shrinkage 24 or low pressure turbine 32 one installed rotor support system 100. Therefore, it should be understood that the rotor support system 100 can The compressor section, turbine section or part of the combustion section of a gas turbine engine 10. Rotating drum rotor 102 can be supported by the rotor support system 100 (for example, through one Or multiple bearing components 106) supports within the engine 10. In such an embodiment, each bearing component 106 can be

constructed from the structural non -rotating support shell of the gas turbine engine 10 that is installed on the outer side of the rotary drum 102. Rotary 102. For example, as shown in Figure 2, bearing component 106 can be positioned in the rotor support

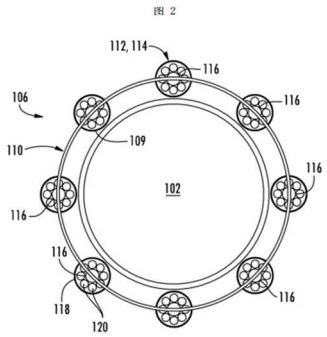

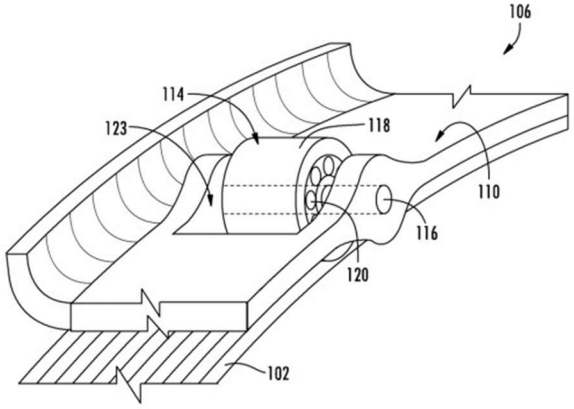

system
100 rotating drum rotation 102 and the support shell 108. Therefore, in one embodiment, as shown in the figure, bearing component 106 can be positioned at 107 back end of the rotating drum 102, which can rotate the drum -shaped rotor 102 can be a general upper cantilever. In another embodiment, the bearing component 106 can be located along the rotating drum rotor 102 at any or more axial position.
As shown in Fig.2, the rotor support system. The Tong 100 can typically include a rotatable drum rotor 102 which is constructed to support multiple blades extending inward from its radial direction. Each of Roller Bearing 114 Elvispy Lanca 123 in a fixed support frame 110Inside. In such an embodiment, a fixed inner seat 116 of a single roller bearing 114 or every one in the support shaft can be solid toThe relative side of the empty cavity 123 within the fixed support frame 110. In the alternative embodiment, as shown in Figure 5, the fixed support frame 110 can be a simple ring, fixed inner seat 116 or each of the support shaft is fixed to the fixed support frame 110 at the end of its end. Now the reference map shows the local perspective of another embodiment of the fixed support framework 110. As shown in the figure, the fixed support framework 110 may include installation or other ways to be solid to one or more fixed arm components 127 of one or more fixed arm components of the unable to rotate support shell 108, and can be extended from the inner seat 116. In addition, as shown in the figure, the roller bearing is supported on one side (for example, via cantilever support parts). In other embodiments, the roller bearings can also be kept on both sides.

1.4 Bearing failure factors and health monitoring of electrical machines

acknowledged reviews on the failure of electrical machines, such as starters and generators, report that bearings account for 40-50 % of all failures. This high incidence has sparked a number of diagnostic studies, which are largely based on the use of current measurement analysis and signal processing techniques, e.g., studies by Benbouzid and Elbou chikhi . Nandy also reported that although in-service conditions such as vibration, inherent eccentricity and electrical currents can negatively affect bearing performance, other external factors can have an even stronger influence on bearing premature failure, namely: • Contamination and corrosion - caused by pitting and sanding action of hard abrasive minute particles or corrosive action of water, acid, etc.; • Improper lubrication - both under and over lubrication can cause abrasion and heating; • Improper installation - poor installation practices can result in misalignment

and eventually pitting or brinelling. Tandon conducted a diagnostic study on electrical machines to determine the most sensitive sensors for bearing fault detection. A range of monitoring techniques that included electrical signatures monitoring, vibration, acoustic emissions (AE), and shock pulse method (SPM) were compared. Those tests consisted in running induction motors fitted with conventional steel bearings with seeded defects on the outer raceways. The size of the defects varied from 250 μm to 1.5 mm, while the load also varied from 0 to 27 kg at a constant speed of 1400 rpm. Results were expressed as a function of the signal percentage increase with respect to average of healthy bearing, for the smallest defect. Their experiments showed that both AE and SPM measurements had a considerable higher response than other techniques. Those results are invaluable for our research since they identify the most effective sensors for earliest detection: AE and analysis of high frequency vibrations. 2.3 Bearing health management algorithm review Unlike conventional rolling element bearings, examination of literature on hybrid bearings showed a small number of publications addressing diagnosis and prognosis . Significantly, previous research has been done at lower rotational speeds than those envisioned for the newest generation of starter generators (1800 vs. 30,000 rpm). 2.4 Diagnostics and prognostics of hybrid bearings A crucial step for constructing an effective health management system for starter/generators is to employ the appropriate algorithmic approach. The selection of the appropriate algorithms generally responds to the application characteristics, data to be acquired and the algorithm applicability . Algorithm selection can be performed in a heuristic way, using researchers' experience and expertise, or alternatively by Quality Function Deployment (QFD).

1.5 Summary to the solution overview

Modern aircraft require more on-board electrical power than ever before. Increasing the size of starter/generators to provide these additional requirements inevitably increases their mass. Instead, starter/generators manufacturers are considering increasing their operational speed. The rotational speeds of the newer generation of starter/generators are expected to approach 30,000 rpm. This will impose severe loading demands on the currently employed bearings; which can lead to earlier degradation due to harsher rolling contact fatigue (RCF). Additionally, bearings in starter/generators experience severe operational conditions, e.g., extreme temperature, vibration and electrical interference. In response to these new requirements, bearing designers are turning to hybrid bearings for the newest generation of starter/generators. However, not much is known about hybrid bearings wear behavior in this application. Hybrid bearings are typically constructed using rolling elements made of a ceramic material such as silicon nitride, running over fatigue resistant steel raceways. Critically, ceramic materials’ mass can be up to 60 % lower than that of conventional ball bearings, resulting in lower centrifugal loading and skidding （1）. Some of the most recognized performance benefits of hybrid bearings include （2）: higher rotational speed, longer life, lower heat generation and superior starvation tolerance.

CHAPTER 2. DESIGNING OF THE AIRCRAFT ENGINE

2.2. Thermodynamic calculation of gas turbine engine

The following is the Genx_1B74 engine equipped with Boeing 787-8.

The General Electric GEnx ("General Electric Next-generation") is an advanced dual rotor, axial flow, high-bypass turbofan jet engine in production by GE Aviation for the Boeing 787 and 747-8. The GEnx is intended to succeed the CF6 in GE's product line. The purpose of the thermodynamic calculation is to determine the parameters of the working fluid in the typical flow-sections of the installation and specific power, specific fuel consumption, the efficiency of gas turbine engine.[4]

Results of thermodynamic calculation using the following gas-dynamic calculation were provided for determining the geometric parameters of elements and engine as a whole. The necessary data for thermodynamic calculation are: gas temperature before turbine Tg*, compressor pressure ratio πc, ambient pressure

2.2 Selection of operation parameters for the designed engine

Initial data:

$N_e = 1875KW$, $\pi_k{}^* = 10.5$, $T_г{}^* = 1260K$, $T_H = 288K$, $p_H = 101325Pa$ H=0;

Min =0; N_e=2025kW; T_g* =1240 K; π_c^*=10;

σin = 0.98; c = 0.86; t = 0.88; f = 0.97; η(m.t)=0.98 ; Hu=43000 kJ/kg; k = 1,4 ;

R = 287 J/kg K; kg = 1,33.

P_h = 101325Pa, ambient temperature T_h = 288K.

2.3 Determination of the general parameter of the engine

Gas-dynamical calculation of the turbine stage

Pressure ratio of turbine: $\pi_t^* = \frac{p_g^*}{p_t^*} = \frac{1092289}{111458} = 9.8$

Outlet pressure of the turbine:

$P_t^* = (1{,}05 \dots 1.15)P_{atm} = 1.1 \cdot 101325 = 111458$

Outlet temperature of the turbine:

$$T_t^* = T_g^* - \frac{L_{eft}}{\frac{kg}{kg-1}R_g} = 1260 - \frac{609416{,}3}{\frac{1{,}33}{1{,}33-1}287{,}6} = 734{,}1$$

Mass flow rate in combustion chamber (Gg.cc) and turbine (Gg):

$G_g = (1 + g_f)G_{g.cc} = (1 + 0.02049)6{,}571 = 6{,}706$

We accept the velocity coefficient at the inlet of the turbine g =0.265.

$$G_{g.cc} = G_{air}(1 - g_{cooling} - g_{t.aw}) = 6{,}739(1 - 0 - 0.025) = 6{,}571$$

$$q(\lambda_g) = \lambda_g \left(1 - \frac{k_g - 1}{k_g + 1}\lambda_g^2\right)^{\frac{1}{k_g - 1}} \left(\frac{k_g + 1}{2}\right)^{\frac{1}{k_g - 1}} = 0.265 \left(1 - \frac{1.33 - 1}{1.33 + 1} 0{,}265^2\right)^{\frac{1}{1.33 - 1}} \left(\frac{1.33 + 1}{2}\right)^{\frac{1}{1.33 - 1}} = 0.408$$

$$F_g = \frac{G_g\sqrt{T_g^*}}{mp_g^* q(\lambda_g)} = \frac{6{,}706\sqrt{1260}}{0{,}0396 \cdot 945326{,}5 \cdot 0{,}408} = 0{,}015$$

where m = 0.0396.

The height of the blades of the nozzle apparatus of the first stage

$$h_g = \frac{F_g}{\pi \cdot D_{mid\,g}} = \frac{0{,}015}{3{,}14 \cdot 0{,}220} = 0{,}021$$

For multistage turbine

$$D_{mid\,g} = 0.9 Dtip_c = 0.9 \cdot 0.24 = 0.216$$

Tip diameter of inlet turbine

$$D_{tip\,g} = D_{mid\,g} + h_g$$

=0.241 m

Hub diameter of inlet turbine

$$D_{hub\,g} = D_{mid\,g} - h_g = 0.199 \text{ m}$$

We accept the value of the angle of flow in absolute

motion at theoutlet of the turbine

We accept the velocity coefficient at the outlet of the turbine λt =

0.5 and αt = 90°.

And gas dynamic function q(λt)

$$q(\lambda_t) = \lambda_t \left(1 - \frac{k_g - 1}{k_g + 1}\lambda_t\right)^{\frac{1}{k_g - 1}} \left(\frac{2}{k_g + 1}\right)^{\frac{1}{k_g - 1}} = 0.5 \left(1 - \frac{1.33 - 1}{1.33 + 1} 0.5\right)^{\frac{1}{1.33 - 1}} \left(\frac{2}{1.33 + 1}\right)^{\frac{1}{1.33 - 1}} = 0.7121$$

$$F_t = \frac{G_g\sqrt{T_t^*}}{mp_t^* q(\lambda_t) \cdot \sin\alpha_t} = \frac{6{,}706\sqrt{714{,}1}}{0{,}0396 \cdot 111458 \cdot 0{,}71 \cdot 1} = 0.057$$

The height of the blades at the outlet of the turbine

$$D_{mid\,g} = D_{mid\,t}$$

$$h_t = \frac{F_t}{\pi D_{mid\,g}} = \frac{0{,}057}{3{,}14 \cdot 0{,}216} = 0{,}084$$

Tip diameter at the outlet of the turbine

$$D_{tip\,t} = D_{mid\,t} + h_t = 0.220 + 0.084 = 0.3_{04}$$

Hub diameter at the outlet of the turbine

$$D_{hub\,t} = D_{mid\,t} - h_t = 0.220 - 0.084 = 0.136$$

Number of turbine stages

$$z_t = \frac{L_{eft}}{u_{t\,mid} u_{mid}^2 \eta_{mech} \eta_t^*} = \frac{609416,\ 3}{2 \cdot 315^2 \cdot 0{,}98 \cdot 0{,}9} = 3{,}58 \approx 4$$

where μt.mid = 1.2 $u_{mid\,t} = u_c \frac{D_{mid\,t}}{D_{tip\,c}} = 350 \frac{0{,}216}{0{,}24} = 315$

The temperature at the outlet of the fan is determined by the formula:

$$T_{fann} = T_h + \frac{k_a - 1}{k_a \cdot R_a} \cdot L_{fan} = 392.265\,K$$

The pressure at the outlet of the fan is determined by the formula:

$$p_{fann} = \sigma_{sf} \cdot p_h \cdot \pi_{fan} = 0.99 \cdot 100818.375 \cdot Pa \cdot 1.95 = 18754\ Pa$$

The air parameters determination at exit from secondary flow jet nozzle

$$T_{fd2} = T_{fann} = 392.265K$$

$$p_{fd2} = p_{fann} = 18754\,Pa$$

Jet velocity of fan air at the jet nozzle is determined by formula for full expansion:

$$c_{fann} = \phi_{fann} \cdot \sqrt{2 \cdot \frac{k_a}{k_a - 1} \cdot R_a \cdot T_{fann} \cdot \left[1 - \left(\frac{P_h}{p_{fann}}\right)^{\frac{k_a - 1}{k_a}}\right]} = 307.254 \frac{m}{s}$$

where $\phi_{fann} = 0.975$ is velocity coefficient of the secondary flow jet nozzle

Static pressure and static temperature at the secondary flow jet nozzle are:

$$p_{fannst} = P_h = 101325\,Pa$$

$$T_{fannst} = T_{fann} - \frac{k_a - 1}{k_a \cdot R_a \cdot 2} \cdot c_{fann}^{\ 2} = 319.15\,K$$

2.3.1 The air parameters determination behind the compressor

Efficiency is determined by the formula:

$$\eta_c = \frac{\pi_c^{\frac{k_a - 1}{k_a}} - 1}{\pi_c^{\frac{k_a - 1}{k_a \cdot \eta_{st}}} - 1} = \frac{35^{\frac{1.4 - 1}{1.4}} - 1}{35^{\frac{1.4 - 1}{1.4 \cdot 0.91}} - 1} = 0.827$$

where $\eta_{st} = 0.91$ is efficiency of the compressor stage;

The work of air compression in the compressor can be calculated as follow:

The total air pressure behind the compressor:

$$p_{cd} = p_h \cdot \pi_c = 100818.375 \cdot Pa \cdot 35 = 3.72 \times 10^6 Pa$$

The total air temperature behind the compressor

$$T_{cd} = T_h + \frac{k_a - 1}{k_a} \cdot \frac{L_{comp}}{R_a} = 288 \cdot K + \frac{1.4 - 1}{1.4} \cdot \frac{579830.16 \cdot m^2 \cdot s^{-2}}{287.3 \cdot \frac{J}{kg \cdot K}} = 813.79 K$$

2.3.3 The gas parameters determination behind the combustion chamber

The temperature before turbine is: $T_{ti} = T_g = 1500 K$

The pressure before turbine is:

$$p_{ti} = p_{cd} \cdot \sigma_{cc} = 2.52 \times 10^6 \cdot Pa \cdot 0.98 = 2.47 \times 10^6 Pa$$

where $\sigma_{cc} = 0.98$

Average specific heat of gases in combustion chamber is determined by the formula:

$$c_{pav} = 878 \frac{J}{kg \cdot K} + 0.208 \frac{J}{kg \cdot K^2} \cdot \left(T_{ti} + 0.48 \cdot T_{cd}\right) = 1343.910 \cdot \frac{J}{kg \cdot K}$$

Relative fuel consumption in the combustion chamber is determined by the formula:

$$g_f = \frac{c_{pav} \cdot \left(T_{ti} - T_{cd}\right)}{\eta_{cc} \cdot H_u} = \frac{1343.910 \cdot m^2 \cdot K^{-1} \cdot s^{-2} \cdot (1500 \cdot K - 813.79 \cdot K)}{0.995 \cdot 42 \cdot 10^6 \cdot \frac{J}{kg}} = 0.027$$

where $H_u = 42 \cdot 10^6 \frac{J}{kg}$

Average excess air/fuel ratio in combustion chamber:

$$\alpha = \frac{1}{g_f \cdot l_0} = \frac{1}{0.027 \cdot 14.9} = 2.784$$

where $l_0 = 14.9$ is mass of air needed for full fuel ignition with the mass of 1 kg.

2.3.3The gas parameters determination behind the turbine

Effective work of all stages of the turbine is determined by the following equation:

$$L_t = \frac{m_f \cdot L_{fan} + L_{comp}}{\left(1 + g_f\right) \cdot \left(1 - g_{cool}\right) \cdot \eta_m} = 91376.304 \cdot \frac{J}{kg}$$

where $g_{cool} = 0.08$ is relative consumption of air, which selected on the exit of the compressor, for cooling of details of the turbine; $\eta_m = 0.995$ is mechanical efficiency

Air temperature at the outlet of the turbine is determined by the formula:

$$T_{td} = T_{ti} - \frac{k_g - 1}{k_g} \cdot \frac{L_t}{R_g} = 1500 \cdot K - \frac{1.333 - 1}{1.333} \cdot \frac{91376.304 \cdot m^2 \cdot s^{-2}}{288 \cdot \frac{J}{kg \cdot K}} = 736.367\,K$$

Air pressure at the outlet of the turbine is determined by the formula:

$$p_{td} = p_{ti} \cdot \left(1 - \frac{T_{ti} - T_{td}}{T_{ti} \cdot \eta_t}\right)^{\frac{k_g}{k_g - 1}} = 131976.234$$

where $\eta_t = 0.9$ is efficiency of the compressor's drive turbine

2.3.4 Gas parameters determination at the exit from the primary flow jet nozzle

Jet nozzle pressure ratio:

$$\pi_n = \frac{p_{td}}{p_h} = \frac{131976.234Pa}{100818.375 \cdot Pa} = 1.309$$

comparing with critical one, $\pi_{ncr} = 1.85$ we have subsonic nozzle.

Nozzle gas velocity is:

$$c_n = \phi_n \cdot \sqrt{2 \cdot \frac{k_g}{k_g - 1} \cdot R_g \cdot T_{td} \cdot \left[1 - \left(\frac{P_h}{p_{td}}\right)^{\frac{k_g - 1}{k_g}}\right]} = 225.321\,\frac{m}{s}$$

where $\phi_n = 0.975$

Gas temperature at the outlet of the power turbine is determined by the formula:

$$T_{nst} = T_{td} - \frac{k_g - 1}{k_g} \cdot \frac{c_n^2}{2 \cdot R_g} = 775.2 \cdot K - \frac{1.3 - 1}{1.3} \cdot \frac{\left(217 \cdot m \cdot s^{-1}\right)^2}{2 \cdot 288 \cdot \frac{J}{kg \cdot K}} = 754.8\,K$$

Gas pressure at the outlet of the power turbine is determined by the formula:

$$p_{nst} = P_h = 101325\,Pa$$

2.4 Calculation of specific parameters

Specific thrust of the primary flow at $V = 0$

$$P_{sp1} = c_n \cdot \left(1 + g_f\right) - V = 225.321 \cdot m \cdot s^{-1} \cdot (1 + 0.027) - 0 = 231.447\,\frac{m}{s}$$

Specific thrust of the secondary flow

$$P_{sp2} = c_{fann} - V = 289.266 \cdot m \cdot s^{-1} - 0 = 289.266\,\frac{m}{s}$$

Total specific thrust:

$$P_{sp} = \frac{P_{sp1} + m_f \cdot P_{sp2}}{1 + m_f} = \frac{231.447 \cdot m \cdot s^{-1} + 5.5 \cdot 289.266 \cdot m \cdot s^{-1}}{1 + 5.5} = 287.935 \frac{m}{s}$$

Specific fuel consumption is:

$$C_{sp} = \frac{3600 m \cdot s^{-1} \cdot g_f \cdot (1 - g_{cool}) \cdot kg}{P_{sp} \cdot (1 + m_f) \cdot N \cdot hr} = 0.03524 \cdot \frac{kg}{N \cdot hr}$$

The total mass flow rate of air passing through engine:

$$G_a = \frac{P}{P_{sp}} = \frac{310 \cdot 10^3 \cdot N}{287.935 \cdot m \cdot s^{-1}} = 1076.632 \frac{kg}{s}$$

The primary mass flow rate of air:

$$G_{a1} = \frac{G_a}{1 + m_f} = \frac{1076.632 \cdot kg \cdot s^{-1}}{1 + 5.5} = 165.636 \frac{kg}{s}$$

The secondary mass flow rate of air:

$$G_{a2} = \frac{m_f}{1 + m_f} \cdot G_a = \frac{5.5}{1 + 5.5} \cdot 1076.632 \cdot kg \cdot s^{-1} = 910.996 \frac{kg}{s}$$

Thermodynamic efficiency of the engine is:

$$\eta_{internal} = \frac{P_{sp1}^2 + m_f \cdot P_{sp2}^2}{2 \cdot g_f \cdot H_u \cdot (1 - g_{cool})} = 0.3597 asd$$

2.5 Gas dynamic calculation of gas turbine engine

The purpose of gas-dynamic calculation is to determine the size of typical cross sections of flow part of the rotors and the frequency of their rotation, the number of compressor and turbine stages, distribution of the compression (expansion) between the stages and degrees, clarify the parameters of GTE. During the gas-dynamic calculation based on selection of axial velocity component of air at the inlet to the compressor C1a. These parameters largely determine the size diametrically GTE, the number of degrees of compressor and turbine, and axial dimensions.[5]

2.5.1 The fan inlet diametric dimensions determination

Reduced velocity λ1a is:

$$\lambda_{1a} = \frac{c_{1a}}{c_{1cr}} = \frac{220 \cdot \frac{m}{s}}{310.561 \cdot m \cdot s^{-1}} = 0.708$$

where $c_{1a} = 220 \frac{m}{s}$ is circular speed at the inlet of compressor.

Relative density is determined by formula:

$$q(\lambda) = \left(\frac{k_a + 1}{2}\right)^{\frac{1}{k_a - 1}} \cdot \lambda \cdot \left(1 - \frac{k_a - 1}{k_a + 1} \cdot \lambda^2\right)^{\frac{1}{k_a - 1}} \qquad q(\lambda_{1a}) = 0.898$$

The area of flowing part at the inlet of fan is determined by the formula:

$$F_{fi} = \frac{G_a \cdot \sqrt{T_h}}{m_a \cdot p_h \cdot q(\lambda_{1a})} = \frac{1076.32 \cdot kg \cdot s^{-1} \cdot \sqrt{288 \cdot K}}{0.04 \cdot \frac{\sqrt{K} \cdot s}{m} \cdot 100818.375 \cdot Pa \cdot q(0.708)} = 4.138\,m^2$$

The first stage relative diameter is: $d_{11} = 0.3$

Fan inlet tip diameter is determined as:

$$D_{1ft} = \sqrt{\frac{4 \cdot F_{fi}}{\pi \cdot \left(1 - d_{11}^2\right)}} = \sqrt{\frac{4 \cdot 4.138 \cdot m^2}{3.142 \cdot \left(1 - 0.3^2\right)}} = 2.574\,m$$

Fan inlet sleeve diameter is determined as:

$$D_{1sl} = \sqrt{D_{1ft}^2 - \frac{4 \cdot F_{fi}}{\pi}} = \sqrt{(2.574 \cdot m)^2 - \frac{4 \cdot 4.138 m^2}{3.142}} = 0.872\,m$$

Area of the secondary flow is:

$$F_2 = F_{fi} \cdot \frac{G_{a2}}{G_a} = 4.138 \cdot m^2 \cdot \frac{910.996 \cdot kg \cdot s^{-1}}{1076.632 \cdot kg \cdot s^{-1}} = 3.49\,m^2$$

Diameter of division of the flow is:

$$D_1 = \sqrt{D_{1ft}^2 - \frac{F_2 \cdot 4}{\pi}} = \sqrt{(2.574 \cdot m)^2 - \frac{3.241 \cdot m^2 \cdot 4}{3.142}} = 1.14\,m$$

2.5.2 Determination of fan stages number

Circumferential velocity on D1 is equal to:

$$u_1 = u_{1ft} \cdot \frac{D_1}{D_{1ft}} = 500 \cdot \frac{m}{s} \cdot \frac{1.14 \cdot m}{2.137 \cdot m} = 266.729\,\frac{m}{s}$$

Circumferential velocity on sleeve diameter is equal to:

$$u_{1sl} = u_{1ft} \cdot \frac{D_{1sl}}{D_{1ft}} = 500 \cdot \frac{m}{s} \cdot \frac{0.916 \cdot m}{2.137 \cdot m} = 214.319\,\frac{m}{s}$$

The air swirl in rotor blades on diameter D1 and near the sleeve can be calculated by the formula:

$$\Delta W_{usl} = c_{1a} \cdot \frac{1.55}{1 + 1.5 \cdot bt_{sl}^{-1}} = 220 \cdot \frac{m}{s} \cdot \frac{1.55}{1 + 1.5 \cdot 2.2^{-1}} = 202.757\,\frac{m}{s}$$

$$\Delta W_{u1} = c_{1a}\cdot\frac{1.55}{1+1.5\cdot\frac{1}{bt_1}} = 220\cdot\frac{m}{s}\cdot\frac{1.55}{1+1.5\cdot\frac{1}{1.376}} = 163.161\,\frac{m}{s}$$

where $bt_{sl} = 2.2$ and $bt_1 = 1.376$

The work on diameter D1 and near the sleeve can be calculated by Euler's equation:

$$L_1 = u_1\cdot\Delta W_{u1} = 266.729\cdot m\cdot s^{-1}\cdot 163.161\cdot m\cdot s^{-1} = 43519.77\cdot\frac{J}{kg}$$

$$L_{1sl} = u_{1sl}\cdot\Delta W_{usl} = 214.319\cdot m\cdot s^{-1}\cdot 202.757\cdot m\cdot s^{-1} = 43454.678\cdot\frac{J}{kg}$$

$$L_{fan1} = \frac{1}{2}\cdot\left(L_1 + L_{1sl}\right) = \frac{1}{2}\cdot\left(43519.77+43454.678\cdot m^{2-2}\right) = 43492\cdot\frac{J}{kg}$$

Number of fan stages is:

$$z_{fan1} = \frac{L_{fan1}}{L_{fan}} = \frac{43492\cdot m^2\cdot s^{-2}}{50051.894\cdot m^2\cdot s^{-2}} = 0.869$$

Thus, number of fan stages is $z_{fan} = 1$.

2.5.2 Distribution of compression work between compressor spools and determination of number of high pressure turbine stages of turbofan engine

The work of high pressure compressor can be determined by the formula:

$$L_{hpc} = 0.5\cdot L_{comp} = 0.5\cdot 506029.16\cdot m^2\cdot s^{-2} = 253014.58\cdot\frac{J}{kg}$$

The work of high pressure turbine can be determined by the formula:

$$L_{hpt} = \frac{L_{hpc}}{\left(1+g_f\right)\cdot\left(1-g_{cool}\right)\cdot\eta_m} = \frac{253014.58\cdot m^2\cdot s^{-2}}{(1+0.02)\cdot(1-0.08)\cdot 1} = 270574.44\cdot\frac{J}{kg}$$

where $\eta_m = 0.995$ is mechanical efficiency

Loading coefficient of high pressure turbine can be determined by the formula:

$$Y = u_{tmd}\cdot\sqrt{\frac{z\cdot\eta_{hpt}}{2\cdot L_{hpt}}} = 450\cdot\frac{m}{s}\cdot\sqrt{\frac{0.89}{2\cdot 270574.439\cdot m^2\cdot s^{-2}}} = 0.577$$

where $z = 1$ is the number of high pressure turbine stages; $u_{tmd} = 450\,\frac{m}{s}$ is circumferential velocity on middle turbine radius; $\eta_{hpt} = 0.89$ is the high pressure turbine efficiency

The work of high pressure turbine stage is:

$$L_{st} = L_{hpt} = 270574.439 \cdot \frac{J}{kg}$$

The work of low pressure compressor is:

$$L_{lpc} = L_{comp} - L_{hpc} - L_{fan} = 202962.687 \cdot \frac{J}{kg}$$

2.5.3 Determination of air parameters and diametric dimensions at the fan exit

For primary airflow axial velocity is:

$$c_{afan1} = c_{1a} - 30\frac{m}{s} = 220 \cdot \frac{m}{s} - 30 \cdot \frac{m}{s} = 190\frac{m}{s}$$

Relative velocity is:

$$\lambda_{afan1} = \frac{c_{afan1}}{18.3\frac{m}{s\sqrt{K}}\sqrt{T_{fd2}}} = \frac{190 \cdot m \cdot s^{-1}}{18.3 \cdot \frac{m}{s \cdot \sqrt{K}} \cdot \sqrt{337.776 \cdot K}} = 0.565$$

Relative density is: $q(\lambda_{afan1}) = 0.777$

Fan outlet area is:

$$F_{fan1} = \frac{G_{a1} \cdot \sqrt{T_{fd2}}}{m_a \cdot p_{fd2} \cdot q(\lambda_{afan1})} = \frac{165.656 \cdot kg \cdot s^{-1} \cdot \sqrt{337.776\,K}}{0.04 \cdot \frac{\sqrt{K} \cdot s}{m} \cdot 164686.816 \cdot Pa \cdot 0.777} = 0.512 \cdot m^2$$

Fan sleeve diameter:

$$D_{fansl} = D_{1sl} = 0.916\,m$$

Fan outer diameter is:

$$D_{fan1} = \sqrt{D_{fansl}^2 + \frac{4 \cdot F_{fan1}}{\pi}} = \sqrt{(0.916 \cdot m)^2 + \frac{4 \cdot 0.512 \cdot m^2}{3.142}} = 1.379\,m$$

For secondary airflow:

The fan outlet axial air speed:

$$c_{afan2} = c_{fann} - 10\frac{m}{s} = 289.266 \cdot m \cdot s^{-1} - 10 \cdot \frac{m}{s} = 279.266\frac{m}{s}$$

Relative velocity is:

$$\lambda_{afan2} = \frac{c_{afan2}}{18.3\frac{m}{s \cdot \sqrt{K}}\sqrt{T_{fann}}} = \frac{279.266 \cdot m \cdot s^{-1}}{18.3 \cdot \frac{m}{s \cdot \sqrt{K}} \cdot \sqrt{337.776 \cdot K}} = 0.83$$

Relative density is: $q(\lambda_{afan2}) = 0.983$

Fan outlet area is:

$$F_{fan2} = \frac{G_{a2}\cdot\sqrt{T_{fann}}}{m_a\cdot p_{fd2}\cdot q\left(\lambda_{afan2}\right)} = \frac{910.996\cdot kg\cdot s^{-1}\cdot\sqrt{337.776\cdot K}}{0.04\cdot\frac{\sqrt{K}\cdot s}{m}\cdot 164686.816\cdot Pa\cdot 0.965} = 2.367 m^2$$

The internal fan exit diameter is:

$$D_2 = D_{fan1} + \delta = 1.379\cdot m + 15\cdot 10^{-3}\cdot m = 1.394 m$$

where $\delta = 0.015\,m$ is width of separating wall.

The external fan exit diameter is:

$$D_{fan2} = \sqrt{D_2^2 + \frac{4}{\pi}\cdot F_{fan2}} = \sqrt{D_2^2 + \frac{4}{\pi}\cdot F_{fan2}} = 2.894\,m$$

2.5.4 Determination of diametric sizes at entry of the low pressure compressor

Pressure ratio of the low pressure compressor:

$$\pi_{lpc} = \left(1 + \frac{L_{lpc}\cdot\eta_{fan}}{\frac{k_a\cdot R_a}{k_a - 1}\cdot T_{fann}}\right)^{\frac{k_a}{k_a-1}} = \left(1 + \frac{202962.7\cdot m^2\cdot s^{-2}\cdot 0.9}{\frac{1.4\cdot 287.3\cdot\frac{J}{kg\cdot K}\cdot 337.8\cdot K}{1.4-1}}\right)^{\frac{1.4}{1.4-1}} = 4.7$$

The total air temperature becomes:

$$T_{lpcd} = T_{fann} + \frac{k_a - 1}{k_a\cdot R_a}\cdot L_{lpc} = 547.6\,K$$

The total air pressure becomes:

$$p_{lpcd} = \pi_{lpc}\cdot p_{fann} = 4.7\cdot 164686.816\cdot Pa = 732651.614\,Pa$$

The low pressure compressor inlet axial air speed: $c_{alpc} = 150\frac{m}{s}$

Relative velocity is:

$$\lambda_{alpc} = \frac{c_{alpc}}{18.3\frac{m}{s\cdot\sqrt{K}}\sqrt{T_{fann}}} = \frac{150\cdot\frac{m}{s}}{18.3\cdot\frac{m}{s\cdot\sqrt{K}}\cdot\sqrt{337.776\cdot K}} = 0.446$$

Relative density is: $q\left(\lambda_{alpc}\right) = 0.647$

Low pressure compressor inlet area is:

$$F_{lpci} = \frac{G_{a1}\cdot\sqrt{T_{fann}}}{m_a\cdot p_{fann}\cdot\sigma_{icc}\cdot q\left(\lambda_{alpc}\right)} = \frac{126.89\cdot kg\cdot s^{-1}\cdot\sqrt{337.78\cdot K}}{0.04\cdot\frac{\sqrt{K}\cdot s}{m}\cdot 164686.82\cdot Pa\cdot 0.99\cdot 0.65} = 0.62\,m^2$$

$\sigma_{icc} = 0.99$ is pressure recovery coefficient

Low pressure compressor sleeve diameter is:

$$D_{1lpcsl} = D_{fansl} = 0.62\,m$$

Low pressure compressor tip diameter is:

$$D_{1lpc} = \sqrt{D_{1lpcsl}^2 + \frac{4}{\pi}\cdot F_{lpci}} = \sqrt{(0.62\cdot m)^2 + \frac{4}{3.142}\cdot 0.62\cdot m^2} = 1.014\,m$$

2.6 Determination of air parameters and diametric sizes

The low pressure compressor exit axial air speed: $c_{lpcd} = 130 m\cdot s^{-1}$;

Relative velocity is:

$$\lambda_{lpcd} = \frac{c_{lpcd}}{18.3\frac{m}{s\cdot\sqrt{K}}\cdot\sqrt{T_{lpcd}}} = \frac{130\cdot m\cdot s^{-1}}{18.3\cdot\frac{m}{s\cdot\sqrt{K}}\cdot\sqrt{547.6\cdot K}} = 0.327$$

Relative density is: $q(\lambda_{lpcd}) = 0.464$

Low pressure compressor discharge area is:

$$F_{lpcd} = \frac{G_{a1}\cdot\sqrt{T_{lpcd}}}{m_a\cdot p_{lpcd}\cdot q(\lambda_{lpcd})} = \frac{126.886\cdot kg\cdot s^{-1}\cdot\sqrt{539.6\cdot K}}{0.04\cdot\frac{\sqrt{K}\cdot s}{m}\cdot 732651.614\cdot Pa\cdot 0.464} = 0.236\,m^2$$

Low pressure compressor sleeve exit diameter:

$$D_{lpcsl} = D_{1lpcsl} = 0.695\cdot m = 0.695\,m$$

Low pressure compressor tip exit diameter:

$$D_{1lpcd} = \sqrt{D_{lpcsl}^2 + \frac{4}{\pi}\cdot F_{lpcd}} = \sqrt{(0.695\cdot m)^2 + \frac{4}{3.142}\cdot 0.236\cdot m^2} = 0.95\,m$$

Low pressure compressor exit blade height:

$$h_{lpcb} = \frac{D_{1lpcd} - D_{lpcsl}}{2} = \frac{0.95\cdot m - 0.695\cdot m}{2} = 255\cdot mm$$

Blade height must be not less than 17mm

2.6.1 Determination of diametric sizes at the entry of the high pressure compressor

The high pressure compressor inlet axial air speed: $c_{ahpc} = 130 m\cdot s^{-1}$;

Relative velocity is:

$$\lambda_{ahpc} = \frac{c_{ahpc}}{18.3\frac{m}{s\cdot\sqrt{K}}\sqrt{T_{lpcd}}} = \frac{130\cdot m\cdot s^{-1}}{18.3\cdot\frac{m}{s\cdot\sqrt{K}}\cdot\sqrt{539.618\cdot K}} = 0.306$$

Relative density is: $q(\lambda_{ahpc}) = 0.464$

High pressure compressor inlet area is:

$$F_{hpci} = \frac{G_{a1}\cdot\sqrt{T_{lpcd}}}{m_a\cdot p_{lpcd}\cdot\sigma_{icc}\cdot q(\lambda_{ahpc})} = \frac{126.89\cdot kg\cdot s^{-1}\cdot\sqrt{539.62\cdot K}}{0.04\cdot\frac{\sqrt{K}\cdot s}{m}\cdot 732651.61\cdot Pa\cdot 0.99\cdot 0.46} = 0.22\,m^2$$

High pressure compressor tip inlet diameter:

$$D_{1hpc} = D_{1lpcd} = 0.87\,m$$

High pressure compressor sleeve inlet diameter:

$$D_{1hpcsl} = \sqrt{D_{1hpc}^2 - \frac{4}{\pi}\cdot F_{hpci}} = \sqrt{(0.87\cdot m)^2 - \frac{4}{3.142}\cdot 0.217\cdot m^2} = 0.693\,m$$

High pressure compressor inlet blade height:

$$h_{hpci} = \frac{D_{1hpc} - D_{1hpcsl}}{2} = \frac{0.87\cdot m - 0.693\cdot m}{2} = 88.499\cdot mm$$

2.6.2 Determination of air parameters and diametric sizes at the high pressure compressor exit

The temperature of air at the exit from HPC is: $T_{cd1} = T_{cd} = 791.236\,K$

Pressure ratio of HPC is:

$$\pi_{hpc} = \frac{p_{cd}}{p_{lpcd}\cdot\sigma_{icc}} = \frac{2.52\times 10^6\cdot Pa}{732651.614\cdot Pa\cdot 0.99} = 3.475$$

The high pressure compressor discharge axial air speed: $c_{acd} = 150\frac{m}{s}$

Relative velocity is: $\lambda_{acd} = 0.291$

Relative density is: $q(\lambda_{acd}) = 0.444$

High pressure compressor discharge area is:

$$F_{cd} = \frac{G_{a1}\cdot\sqrt{T_{cd1}}}{m_a\cdot p_{cd}\cdot q(\lambda_{acd})} = \frac{126.886\cdot kg\cdot s^{-1}\cdot\sqrt{791.236\cdot K}}{0.04\cdot\frac{\sqrt{K}\cdot s}{m}\cdot 2.52\times 10^6\cdot Pa\cdot 0.444} = 0.079\,m^2$$

High pressure compressor sleeve exit diameter:

$$D_{slhpcd} = 0.81\ m$$

High pressure compressor tip exit diameter:

$$D_{1hpcd} = \sqrt{D_{slhpcd}^{2} + \frac{4}{\pi}\cdot F_{cd1}} = \sqrt{(0.81\cdot m)^{2} + \frac{4}{3.142}\cdot 0.079\cdot m^{2}} = 0.87\,m$$

High pressure compressor discharge blade height:

$$h_b = \frac{D_{1hpcd} - D_{slhpcd}}{2} = \frac{0.87\cdot m - 0.81\cdot m}{2} = 29.999\cdot mm$$

2.6.3 Determination of diametric sizes at the entry to the high pressure turbine

Jet velocity of gas emission from the first nozzle diaphragm is determined by Euler equation, on the assumption of axial outlet from the first turbine wheel of high-pressure turbine being:

$$c_1 = \frac{L_{hpt}}{u_{tmd}\cdot\cos\left(\frac{\pi}{180}\cdot\alpha_1\right)} = \frac{270574.439\cdot m^{2}\cdot s^{-2}}{450\cdot\frac{m}{s}\cdot\cos\left(\frac{3.142}{180}\cdot 25\right)} = 663.436\frac{m}{s}$$

where $\alpha_1 = 25$ is the angle of a stream output from the ND

Relative velocity is:

$$\lambda_1 = \frac{c_1}{18.15\cdot\frac{m}{s\sqrt{K}}\sqrt{T_{ti}}} = \frac{663.436\cdot m\cdot s^{-1}}{18.15\cdot\frac{m}{s\cdot\sqrt{K}}\cdot\sqrt{1500\cdot K}} = 0.944$$

Relative density is: $q_g(\lambda_1) = 0.996$

Mass gas flow rate through the first stages ND is determined by the formula:

$$G_{gti} = G_{a1}\cdot(1 + g_f)\cdot(1 - g_{cool1}) = 126.89\cdot kg\cdot s^{-1}\cdot(1 + 0.02)\cdot(1 - 0.08) = 119.04\frac{k}{s}$$

where $g_{cool1} = 0.082$ is relative consumption of compressor-bleed air for cooling parts of HPT.

The section area of turbine air-gas channel at exit from ND is calculated by equation:

$$F_{1nd} = \frac{G_{gti}\cdot\sqrt{T_{ti}}}{m_g\cdot p_{ti}\cdot\sigma_{nd}\cdot q_g(\lambda_1)\cdot\sin\left(\frac{\pi}{180}\cdot\alpha_1\right)} = 0.115\,m^{2}$$

where $\sigma_{nd} = 0.97$ is the total pressure recovery coefficient in the ND.

Turbine mean diameter is equal to:

$$D_{tmd} = 0.774\,m$$

Blade height of the high pressure turbine inlet:

$$h_{blti} = \frac{F_{1nd}}{\pi \cdot D_{tmd}} = \frac{0.115 \cdot m^2}{3.142 \cdot 0.735 \cdot m} = 0.05\,m$$

Tip diameter of high pressure turbine inlet is:

$$D_t = D_{tmd} + h_{blti} = 0.735 \cdot m + 0.05 \cdot m = 0.785\,m$$

Sleeve diameter of high pressure turbine inlet is:

$$D_{sl} = \sqrt{D_t^2 - \frac{4}{\pi} \cdot F_{1nd}} = \sqrt{(0.785 \cdot m)^2 - \frac{4}{3.142} \cdot 0.115 \cdot m^2} = 0.715\,m$$

2.6.4 Determination of diametric sizes at the high pressure turbine exit

The total gas temperature at the exit from HPT is determined by the formula:

$$T_{hptd} = T_{ti} - \frac{k_g - 1}{k_g} \cdot \frac{L_{hpt}}{R_g} = 1500 \cdot K - \frac{1.33 - 1}{1.33} \cdot \frac{270574.44 \cdot m^2 \cdot s^{-2}}{288 \cdot \frac{J}{kg \cdot K}} = 1273.5\,K$$

The total gas pressure at the exit from HPT is determined by the formula:

$$p_{hptd} = p_{ti} \cdot \left(1 - \frac{T_{ti} - T_{hptd}}{T_{ti} \cdot \eta_{hptd}}\right)^{\frac{k_g}{k_g - 1}} = 1.367 \times 10^6\,Pa$$

Axial velocity at the exit from the HPT: $ct_1 = 270 \frac{m}{s}$

Relative velocity is: $\lambda_{2a} = 0.418$

Relative density is: $q_g(\lambda_{2a}) = 0.616$

Mass gas flow rate through the exit of HPT is determined by the formula:

$$G_{gtd} = G_{a1} \cdot (1 + g_f) \cdot (1 - g_{cool2}) = 119.87 \frac{kg}{s}$$

Flow part area through HPT exit is:

$$F_{hpt} = \frac{G_{gtd} \cdot \sqrt{T_{hptd}}}{m_g \cdot p_{hptd} \cdot q_g(\lambda_{2a})} = \frac{119.87 \cdot kg \cdot s^{-1} \cdot \sqrt{1265.303 \cdot K}}{0.04 \cdot \frac{\sqrt{K} \cdot s}{m} \cdot 1.217 \times 10^6 \cdot Pa \cdot 0.616} = 0.167\,m^2$$

Blade height is: $h_{bl} = 60mm$

HPT tip discharge diameter is:

$$D_{hptd} = \frac{F_{hpt}}{\pi \cdot h_{bl}} + h_{bl} = \frac{0.167 \cdot m^2}{3.142 \cdot 60 \cdot mm} + 60 \cdot mm = 0.976\,m$$

HPT sleeve discharge diameter is:

$$D_{slhptd} = \frac{F_{hpt}}{\pi \cdot h_{bl}} - h_{bl} = \frac{0.167 \cdot m^2}{3.142 \cdot 60 \cdot mm} - 60 \cdot mm = 0.814m$$

2.6.5 Determination of high pressure compressor stages number

Circumferential speeds on periphery u_{1c}, near the sleeve of the first stage u_{1csl} and near the sleeve of the last stageu_{nsl} are:

$$u_{1c} = u_{tmd} \cdot \frac{D_{1hpc}}{D_{tmd}} = 450 \cdot \frac{m}{s} \cdot \frac{0.945 \cdot m}{0.735 \cdot m} = 547.927 \frac{m}{s}$$

$$u_{1csl} = u_{tmd} \cdot \frac{D_{1hpcsl}}{D_{tmd}} = 450 \cdot \frac{m}{s} \cdot \frac{0.798 \cdot m}{0.735 \cdot m} = 458.457 \frac{m}{s}$$

$$u_{nsl} = u_{tmd} \cdot \frac{D_{slhpcd}}{D_{tmd}} = 450 \cdot \frac{m}{s} \cdot \frac{D_{slhpcd}}{0.735 \cdot m} = 495.835 \frac{m}{s}$$

Choosing the lattice density of the first stage $bt_{sl1} = 1.8$ and for the last stage $bt_{sln} = 1.4$ we can find twisting of air in the first and last stage rotors ΔW_{u1sl} and ΔW_{unsl} and work of the first and last stages:

$$\Delta W_{u1sl} = c_{ahpc} \cdot \frac{1.55}{1 + 1.5 \cdot bt_{sl1}^{-1}} = 130 \cdot m \cdot s^{-1} \cdot \frac{1.55}{1 + 1.5 \cdot 1.8^{-1}} = 109.909 \frac{m}{s}$$

$$\Delta W_{unsl} = c_{acd} \cdot \frac{1.55}{1 + 1.5 \cdot bt_{sln}^{-1}} = 150 \cdot \frac{m}{s} \cdot \frac{1.55}{1 + 1.5 \cdot 1.4^{-1}} = 112.241 \frac{m}{s}$$

$$L_{st1} = u_{1csl} \cdot \Delta W_{u1sl} = 424.173 \cdot m \cdot s^{-1} \cdot 109.909 \cdot m \cdot s^{-1} = 47416.492 \cdot \frac{J}{kg}$$

$$L_{stn} = u_{nsl} \cdot \Delta W_{unsl} = 495.835 \cdot m \cdot s^{-1} \cdot 112.241 \cdot m \cdot s^{-1} = 55862.322 \cdot \frac{J}{kg}$$

$$L_{stav} = \frac{L_{st1} + L_{stn}}{2} = \frac{47416.492 \cdot m^2 \cdot s^{-2} + 55862.322 \cdot m^2 \cdot s^{-2}}{2} = 51874.248 \cdot \frac{J}{kg}$$

Number of compression stages:

$$z_{hpc1} = \frac{L_{hpc}}{L_{stav}} = \frac{253014.58 \cdot m^2 \cdot s^{-2}}{51874.248 \cdot m^2 \cdot s^{-2}} = 4.658$$

Thus, number of HPC stages is: $z_{hpc} = 5$.

Power of HPT and HPC are determined:

$$N_{hpt} = G_{gtd} \cdot L_{hpt} = 119.87 \cdot kg \cdot s^{-1} \cdot 253014.58 \cdot m^2 \cdot s^{-2} = 35.528 \cdot MW$$

$$N_{hpc} = G_{a1} \cdot L_{hpc} = 126.886 \cdot kg \cdot s^{-1} \cdot 253014.58 \cdot m^2 \cdot s^{-2} = 32.104 \cdot MW$$

$$N_{hpt} \cdot \eta_m - N_{hpc} = 32.434 \times 10^6 \cdot W \cdot 0.995 - 32.104 \times 10^6 \cdot W = 0.167 \cdot MW$$

Rotational speed of HPC and HPT are determined by the formulas:

$$n_{hpc} = \frac{2 \cdot u_{1csl}}{D_{1hpcsl}} = \frac{2 \cdot 424.173 \cdot m \cdot s^{-1}}{0.693 \cdot m} = 12769. \cdot rpm$$

$$n_{hpc1} = \frac{2 \cdot u_{tmd}}{D_{tmd}} = \frac{2 \cdot 450 \cdot \frac{m}{s}}{0.735 \cdot m} = 12769. \cdot rpm$$

2.6.6 Determination of low pressure turbine number of stages and distribution of work between them

Mass gas flow rate in LPT is calculated by the formula:

$$G_g = G_{a1} \cdot (1 + g_f) \cdot (1 - g_{coollpt}) = 126.89 \cdot kg \cdot s^{-1} \cdot (1 + 0.02) \cdot (1 - 0.03) = 125.73 \frac{k}{s}$$

Work of LPT is:

$$L_{lpt} = \frac{L_{lpc}}{(1 + g_f) \cdot (1 - g_{coollpt}) \cdot \eta_m} = \frac{297846.43 \cdot m^2 \cdot s^{-2}}{(1 + 0.02) \cdot (1 - 0.03) \cdot 1} = 232245 \cdot \frac{J}{kg}$$

Low pressure turbine loading is equal to:

$$Y_{lpt} = u_{lptmd} \cdot \sqrt{\frac{z_{lpt} \cdot \eta_{lpt}}{2 \cdot L_{lpt}}} = 500 \cdot \frac{m}{s} \cdot \sqrt{\frac{0.88}{2 \cdot 232245 \cdot m^2 \cdot s^{-2}}} = 0.724$$

where $z_{lpt} = 1$ is the number of stages and $\eta_{lpt} = 0.88$ is LPT efficiency.

2.6.7 Determination of diametric sizes at the inlet to the low pressure turbine

Jet velocity is equal:

$$c_2 = \frac{L_{lpt}}{u_{lptmd} \cdot \cos\left(\frac{\pi}{180} \cdot \alpha_2\right)} = \frac{205860.732 \cdot m^2 \cdot s^{-2}}{500 \cdot \frac{m}{s} \cdot \cos\left(\frac{3.142}{180}\right)} = 479.47 \frac{m}{s}$$

The angle $\alpha_2 = 25$

Reduced velocity is:

$$\lambda_2 = \frac{c_2}{18.15 \cdot \frac{m}{s \cdot \sqrt{K}} \cdot \sqrt{T_{hptd}}} = \frac{479.47 \cdot m \cdot s^{-1}}{18.15 \cdot \frac{m}{s \cdot \sqrt{K}} \cdot \sqrt{1265.303 \cdot K}} = 0.704$$

Relative density is: $q_g(\lambda_2) = 0.897$

The section area at the inlet to low pressure turbine is determined by the formula:

$$F_{lpti} = \frac{G_g \cdot \sqrt{T_{hptd}}}{m_g \cdot p_{hptd} \cdot \sigma_{int} \cdot \sigma_{nd} \cdot q_g(\lambda_2) \cdot \sin\left(\frac{\pi}{180} \cdot \alpha_2\right)} = 0.245\,m^2$$

where $\sigma_{int} = 0.985$ and $\sigma_{nd} = 0.97$ are total pressure recovery coefficient in the intermediate case between HPT and LPT, and total pressure recovery coefficient in the ND respectively.

Sleeve diameter of the LPT rotor inlet is:

$$D_{sllpti} = D_{slhptd} \text{ explicit, ALL} = 0.745 \cdot m = 0.745\,m$$

Tip diameter of the LPT rotor inlet is:

$$D_{tlpti} = \sqrt{D_{sllpti}^2 + \frac{4}{\pi} \cdot F_{lpti}} = = 0.906\,m$$

Height of blade is:

$$h_{bllpti} = \frac{D_{tlpti} - D_{sllpti}}{2} = 103.253 \cdot mm$$

2.6.8 Determination of diametric sizes at the inlet to the fan turbine

Jet velocity is equal:

$$c_{f1} = \frac{L_{ft1}}{u_{ftmd} \cdot \cos\left(\frac{\pi}{180} \cdot \alpha_3\right)} = \frac{112029.129 \cdot m^2 \cdot s^{-2}}{216.669 \cdot m \cdot s^{-1} \cdot \cos\left(\frac{3.142}{180} \cdot 25\right)} = 567.253 \frac{m}{s}$$

The angle $\alpha_3 = 25$

Reduced velocity is:

$$\lambda_{f1} = \frac{c_{f1}}{18.15 \cdot \frac{m}{s \cdot \sqrt{K}} \cdot \sqrt{T_{lptd}}} = \frac{567.253 \cdot m \cdot s^{-1}}{18.15 \cdot \frac{m}{s \cdot \sqrt{K}} \cdot \sqrt{1086.738 \cdot K}} = 0.979$$

Relative density is: $q_g(\lambda_{f1}) = 0.997$

$$D_{slft1i} = D_{sllptd} = 0.735\,m$$

Fan turbine inlet tip diameter is:

$$D_{tft1i} = \sqrt{D_{slft1i}^2 + \frac{4}{\pi}\cdot F_{ft1i}} = \sqrt{D_{slft1i}^2 + \frac{4}{\pi}\cdot F_{ft1i}} = 1.53m$$

Fan turbine inlet blade height is:

$$h_{blft1i} = \frac{D_{tft1i} - D_{slft1i}}{2} = \frac{1.53\cdot m - 0.735\cdot m}{2} = 187.236\cdot mm$$

2.6.9 Determination of diametric sizes at the exit from the fan turbine

Temperature of gas after fan turbine is:

$$T_{ftd} = T_{lptd} - \frac{\left(k_g - 1\right)\cdot L_{ft}}{k_g\cdot R_g} = 858.357\,K$$

Pressure of gas after fan turbine is:

$$p_{ftd} = p_{lptd}\cdot\sigma_{int}^{3}\cdot\left(1 - \frac{T_{lptd} - T_{ftd}}{T_{lptd}\cdot\eta_{ft3}}\right)^{\frac{k_g}{k_g - 1}} = 15567.78Pa$$

Reduced velocity is: $\lambda_{3d} = 0.7$

Relative density is: $q_g\left(\lambda_{3d}\right) = 0.894$

Flow area in the zone of fan turbine exit is:

$$F_{ftd} = \frac{G_{gf}\cdot\sqrt{T_{ftd}}}{m_g\cdot p_{ftd}\cdot q_g\left(\lambda_{3d}\right)} = \frac{129.617\cdot kg\cdot s^{-1}\cdot\sqrt{809.096\cdot K}}{0.04\cdot\frac{\sqrt{K}\cdot s}{m}\cdot 15567.78\cdot Pa\cdot 0.894} = 0.935\,m^2$$

Fan turbine exit blade height is:

$$h_{blftd} = 315\cdot mm$$

Fan turbine exit sleeve diameter is:

$$D_{slftd} = \frac{F_{ftd}}{\pi\cdot h_{blftd}} - h_{blftd} = \frac{0.935\cdot m^2}{3.142\cdot 0.271\cdot m} - 0.315\cdot m = 0.873\,m$$

Fan turbine exit tip diameter is:

$$D_{tftd} = \frac{F_{ftd}}{\pi\cdot h_{blftd}} + h_{blftd} = \frac{0.935\cdot m^2}{3.142\cdot 0.271\cdot m} + 0.315\cdot m = 1.452\,m$$

Power balance for fan and fan turbine:

$$N_{ft} = G_{gf} \cdot (L_{ft}) = 188.569 \cdot kg \cdot s^{-1} \cdot L_{ft} = 48.576 \cdot MW$$

$$N_{fan} = G_a \cdot L_{fan} = 1073.759 \cdot kg \cdot s^{-1} \cdot 50051.894 \cdot m^2 \cdot s^{-2} = 47.753 \cdot MW$$

Check:

$$N_{ft} \cdot \eta_m - N_{fan} = 41488193.29 \cdot W \cdot 1 - 41280752.32 \cdot W = 1.003 \cdot W$$

Rotational speeds are:

$$n_{ft} = \frac{2 \cdot u_{ftmd}}{D_{ftmd}} = \frac{2 \cdot 225.917 \cdot m \cdot s^{-1}}{1.003 \cdot m} = 4784.546 \cdot rpm$$

$$n_{fan} = \frac{2 \cdot u_{1ft}}{D_{1ft}} = \frac{2 \cdot 500 \cdot \frac{m}{s}}{2.315 \cdot m} = 4432.457 \cdot rpm$$

2.6.10 Determination of sizes of sections at the exit from jet nozzles

Axial velocities of the primary and secondary flows are:

$$C_{jn1} = \phi_n \cdot \sqrt{\frac{2 \cdot k_g}{k_g - 1} \cdot R_g \cdot T_{ftd} \cdot \left[1 - \left(\frac{P_h}{p_{ftd}}\right)^{\frac{k_g - 1}{k_g}}\right]} = 363.538 \frac{m}{s}$$

$$C_{jn2} = c_{fann} = 289.266 \frac{m}{s}$$

Reduced velocities of the primary and secondary flows are:

$$\lambda_{jn1} = \frac{C_{jn1}}{18.15 \cdot \frac{m}{s \cdot \sqrt{K}} \cdot \sqrt{T_{td}}} = \frac{353.403 \cdot m \cdot s^{-1}}{18.15 \cdot \frac{m}{s \cdot \sqrt{K}} \cdot \sqrt{775.249 \cdot K}} = 0.745$$

$$\lambda_{jn2} = \frac{C_{jn2}}{18.3 \cdot \frac{m}{s \cdot \sqrt{K}} \cdot \sqrt{T_{fann}}} = \frac{289.266 \cdot m \cdot s^{-1}}{18.3 \cdot \frac{m}{s \cdot \sqrt{K}} \cdot \sqrt{337.776 \cdot K}} = 0.876$$

Relative density for primary flow:

$$q_g(\lambda_{jn1}) = 0.785$$

Relative density for secondary flow:

$$q(\lambda_{jn2}) = 0.995$$

Cross sectional are of the primary flow nozzle circle is:

$$Fjn1 = \frac{G_{gf}\cdot\sqrt{T_{ftd}}}{m_g\cdot p_{ftd}\cdot\sigma_{jn1}\cdot q_g\left(\lambda_{jn1}\right)} = \frac{129.62\cdot kg\cdot s^{-1}\cdot\sqrt{809.1\cdot K}}{0.04\cdot\frac{\sqrt{K\cdot s}}{m}\cdot 135729.08\cdot Pa\cdot 0.93\cdot 0.89} = 0.87\ m2$$

Cross sectional are of the secondary flow nozzle circle is:

$$Fjn2 = \frac{G_{a2}\cdot\sqrt{T_{fann}}}{m_a\cdot p_{fann}\cdot\sigma_{sf}\cdot\sigma_{jn2}\cdot q\left(\lambda_{jn2}\right)} = 2.367 m^2$$

Thus, diameters of nozzles are:

$$Djn1 = \sqrt{\frac{4}{\pi}\cdot F_{jn1}} = \sqrt{\frac{4}{3.142}\cdot 0.825\cdot m^2} = 1.345\ m$$

$$Djn2 = \sqrt{\left(Djn1\cdot 1.1\right)^2 + \frac{4}{\pi}\cdot Fjn2} = \sqrt{(1.345\cdot m\cdot 1.1)^2 + \frac{4}{3.14}\cdot 2.367\cdot m2} = 2.6832\ m$$

2.7.1 **Determination of elaborated parameters of the projected engine**

Specific thrust of the primary flow at the complete expansion of gas is

determined by the following equation:

$$PSP1 = Cjn1\cdot\left(1 + g_f\right) - V = 353.403\cdot m\cdot s^{-1}\cdot(1 + 0.022) - 0 = 375.765\ \frac{m}{s}$$

Specific thrust of the secondary flow:

$$PSP2 = Cjn2 - V = 289.266\cdot m\cdot s^{-1} - 0 = 289.266\ \frac{m}{s}$$

Specific thrust of a turbofan engine:

$$PSP = \frac{PSP1 + mf\cdot PSP2}{1 + mf} = \frac{361.009\cdot m\cdot s^{-1} + 5.5\cdot 289.266\cdot m\cdot s^{-1}}{1 + 5.5} = 335.985\ \frac{m}{s}$$

Thrust of turbofan engine:

$$Thrust = PSP\cdot G_a = 300.304\cdot m\cdot s^{-1}\cdot 824.759\cdot kg\cdot s^{-1} = 263.837\cdot kN$$

Specific fuel consumption is:

$$CSP = \frac{g_f\cdot\left(1 - g_{cool}\right)}{P_{SP}\cdot\left(1 + m_f\right)} = \frac{0.02152\cdot(1 - 0.08)}{300.30382\cdot m\cdot s^{-1}\cdot(1 + 5.5)} = 0.03876\cdot\frac{kg}{N\cdot hr}$$

From thermodynamics:

Specific thrust of a turbofan engine: $P_{sp} = 287.935 \cdot \frac{N}{kg \cdot s^{-1}}$

Required thrust: P = 310000 kN

Specific fuel consumption: $C_{sp} = 0.03524 \cdot \frac{kg}{N \cdot hr}$

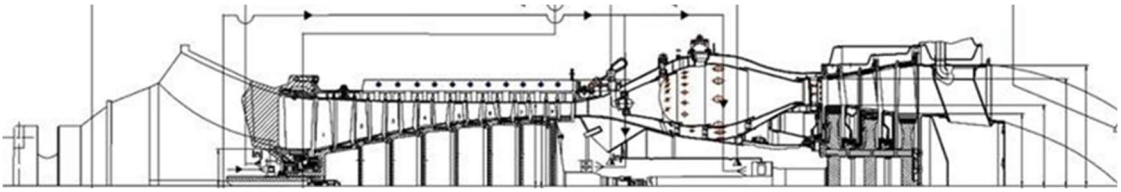

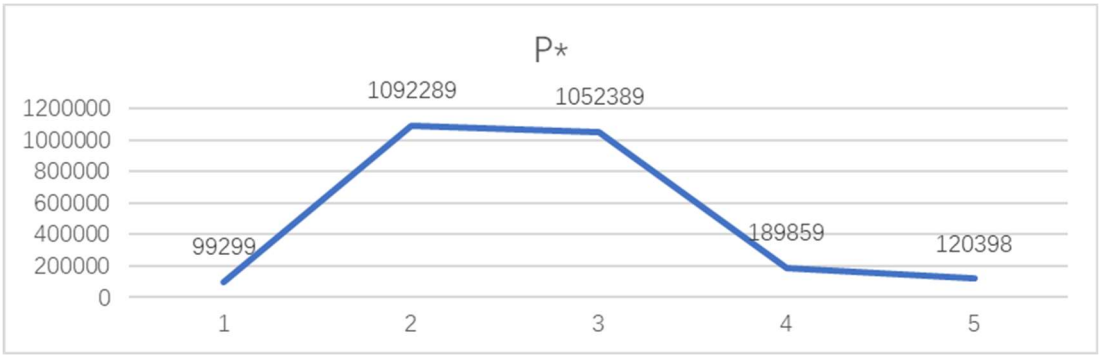

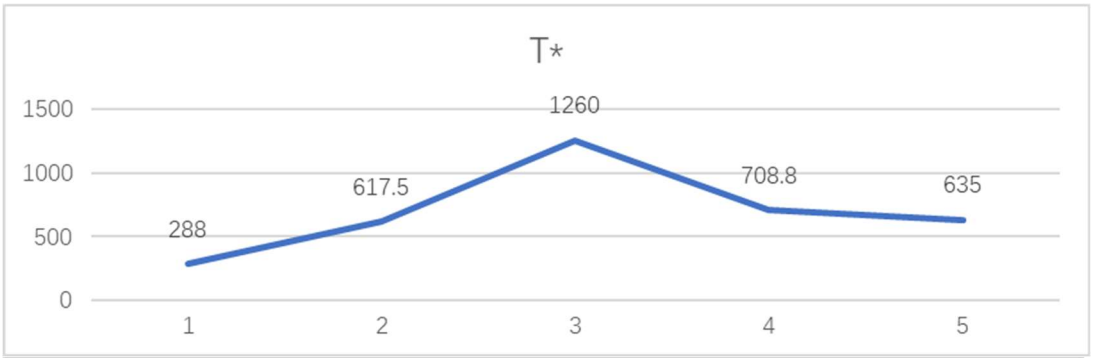

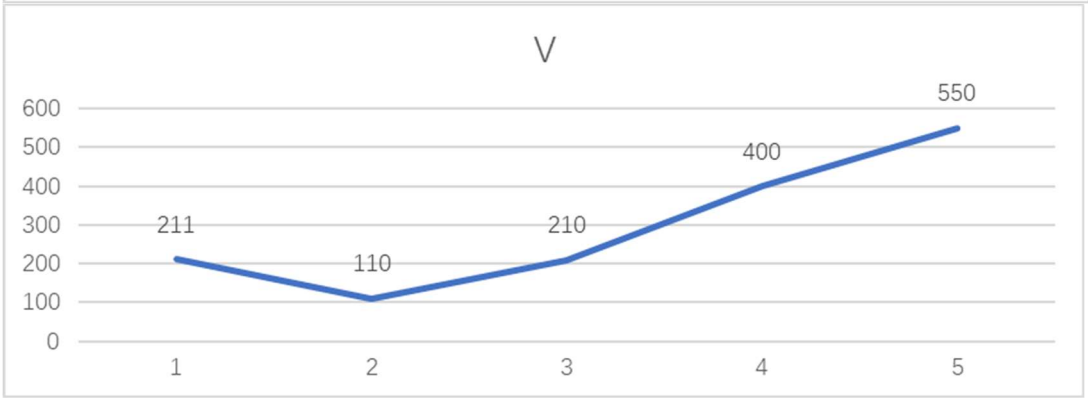

Appendix A

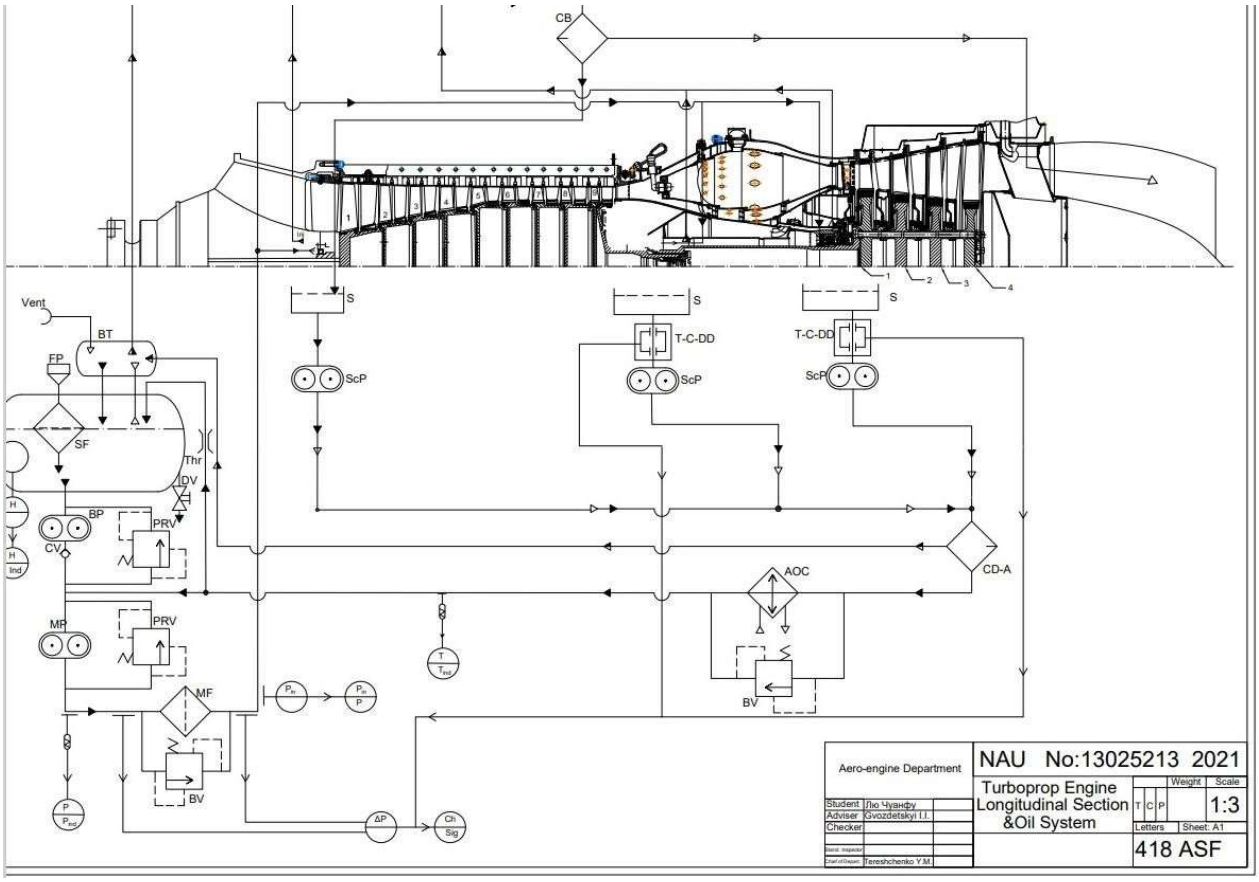

FIG The General Electric GEnx ("General Electric Next-generation") is an advanced dual rotor, axial flow, high-bypass turbofan jet engine

Appendix B

CHAPTER 3 DESIGN FOR SHAFT AND BEARING

3.1 Strength calculation of the high pressure rotor shaft

Turbine shaft perceives all types of stresses that act at engine rotor. These stresses can be divided on internal that are created by rotor elements in engine work process and external which are executed at changing of external factors. Internal of stresses are centrifugal inertial force of unbalanced rotor mass. External stresses that are transferred on rotor from TFE construction elements. At strength shaft calculation are accepted the following deformation which are appeared from action on it static and dynamic forces and moments:

-shaft twisting by action of moment that it transfers;

-shaft bending from own weight, weight of compressor and turbine rotors, centrifugal force of unbalanced rotors mass and also from forces of overloading of compressor and turbine rotors;

-expansion or compression of axial forces that are called the difference of gas pressures by the end of rotor wheels, axial component of inertial forces.

For shafts calculation are chosen the most dangerous incidents their loading when pointed above forces especially the large and are summarized. Such as incidents can be:

-TFE removal on maximum regime;

In the case of multirotor (rotary) gas turbine engine is necessary to carry out the calculation of the high-pressure turbine shaft.[6]

The shaft calculation is necessary to execute in such sequence:

- to draw the calculation scheme with the all necessary dimensions;
- to determine the transversal forces under rotors mass and unbalanced masses;
- to determine the supports reactions under transversal forces for the selected calculation scheme;
- to calculate the gyroscopic moments and supports reactions under their action;
- to build torque moment & bending moment and axial force diagrams;
- to choose the dangerous cross sections;
- to calculate the bending stress by the formula, MPa:

In our case we execute calculation of turbine shaft imponderable at GTP removal at maximum regime.

3.1.1 Mechanical strength calculation

distance from front resistance to the compressor mass center a=0.28

distance from rear resistance to turbine center mass b=0.1m

- distance between supports c=1.0m;
- compressor mass Mc=155 kg;
- turbine mass Mt=68 kg;
- external diameter of turbine shaft D=0.19m;
- limit material flow of turbine shaft $\sigma_{0.2} = 95$ Mpa;
- maximal total moment $M_{\Sigma} = 12000$ N/m

Torque moment:

$$M_{cr} = \frac{9{,}55 \cdot L_{c.h} \cdot G_g}{n_t} = \frac{9{,}55 \cdot L_{c.h} \cdot G_g}{n_t} = \frac{9{,}55 \cdot (2{,}5 \cdot 10^5) \cdot 6{,}706}{4457} = 3{,}6$$

The diameter labyrinth of oil capacity:

$$D_m = 1.1 \cdot D = 1.1 \cdot 0.19 = 0.209 \text{ m}$$

Axial force acting on turbine shaft:

$$Ð_{a.f.} = G_g \cdot (C_1 \cdot sin(\alpha_1) - C_2) + \frac{\pi \cdot (D_{1k}^2 - D_m^2) \cdot P_0}{4} - \frac{\pi \cdot (D_{2k}^2 - D_m^2) \cdot P_2}{4}$$

$$D_{a.f} = 6{,}706(640 \cdot sin(20) - 152) + \frac{3{,}14 \cdot (0{,}232^2 - 0{,}209^2) \cdot 0{,}959 \cdot 10^6}{4} - \frac{3{,}14 \cdot (0{,}33^2 - 0{,}209^2) \cdot 0{,}1115 \cdot 10^6}{4} = 1{,}15 \cdot 10^5$$

Centrifugal force from unbalanced mass compressor:

$$Ð_{u.c} = \frac{G_a \cdot r_c}{g} \cdot \left(\frac{\pi \cdot n_t}{30}\right)^2;$$

$$D_{u.t} = 7{,}42 \cdot 10^5$$

Transverse forces from rotors mass and unbalanced mass:

$$Ð_1 = M_c \cdot g + Ð_{u.c};$$

$$D_1 = 155 \cdot 9{,}81 + 7{,}42 \cdot 10^5 = 7{,}44 \cdot 10^5$$

$$Ð_2 = M_t \cdot g + Ð_{u.t};$$

$$D_2 = 68 \cdot 9{,}81 + 7{,}42 \cdot 10^5 = 7{,}43 \cdot 10^5$$

Support reaction from transverse force:

$$R_À = \frac{Ð_1 \cdot à + Ð_2 \cdot (c + b)}{c};$$

$$R_Â = \frac{Ð_1 \cdot (c - à) - Ð_2 \cdot b}{c};$$

$$R_A = \frac{7{,}44 \cdot 10^5 \cdot 0{,}28 + 7{,}43 \cdot 10^5 \cdot (1{,}0 + 0{,}1)}{1{,}0} = 1{,}03 \cdot 10^6$$

$$R_{A'} = \frac{7{,}44 \cdot 10^5 \cdot (1{,}0 - 0{,}1) + 7{,}43 \cdot 10^5 \cdot 0{,}1}{1{,}0} = 7{,}44 \cdot 10^5$$

Internal turbine shaft:

$$d = 0{,}85 \cdot D$$

$$d = 0{,}85 \cdot 0{,}19 = 0{,}1615$$

Area of shaft intersection:

$$F = \frac{\pi \cdot (D^2 - d^2)}{4};$$

$$F = \frac{3{,}14 \cdot (0{,}19^2 - 0{,}1615^2)}{4} = 7{,}86 \cdot 10^{-3}\ m^2.$$

Stresses of bending:

$$\sigma_{\text{è}} = \frac{M_\Sigma \cdot 32}{\pi \cdot D^3 \cdot \left[1 - \left(\frac{d}{D}\right)^4\right]};$$

$$\sigma_e = \frac{12000 \cdot 32}{3{,}14 \cdot 0{,}19^3 \cdot [1 - (\frac{0{,}1615}{0{,}19})^4} = 3{,}522 \cdot 10^7$$

Extension stresses:

$$\sigma_{ex} = \frac{D_{a.f}}{F};$$

$$\sigma_{ex} = \frac{1{,}15 \cdot 10^5}{7{,}86 \cdot 10^{-3}} = 1{,}46 \cdot 10^7$$

Complex stresses σ_t third of strength theory:

$$\sigma_c = \sqrt{(\sigma_{\text{è}} + \sigma_{ex})^2 + 4 \cdot \tau^2};$$

$$\sigma_c = \sqrt{(3{,}522 \cdot 10^7 + 1{,}46 \cdot 10^7) + 4 \cdot (1{,}865 \cdot 10^7)^2} = 3{,}73 \cdot 10^7$$

Strength safety coefficient:

$$K_{shaft} = \frac{\sigma_{0.2}}{\sigma_c}$$

$$k_{shaft} = \frac{95}{37.3} = 2.55$$

Calculation conclusion: by the request of strength safety coefficient for turbine shafts can be in range 2 ... 3. In our case the shaft executed from steel 40XHMA and minimal of strength safety coefficient is equal: kshaft =2.55 corresponding to request

$$\sigma_{shB} = \frac{32 \cdot M_{B\Sigma}}{\pi \cdot d_{EX}^3 \cdot \left[1 - \left(\frac{d_{IN}}{d_{EX}}\right)^4\right]};$$

of strength in range.

- to calculate the tangent stress by the formula, MPa:

$$\tau_{shtq} = \frac{16 \cdot M_{tq}}{\pi \cdot d_{EX}^3 \cdot \left[1 - \left(\frac{d_{IN}}{d_{EX}}\right)^4\right]};$$

to calculate the tension stress by the formula, MPa:

$$\sigma_T = \frac{4 \cdot P_{AX}}{\pi \cdot d_{EX}^2 \cdot \left[1 - \left(\frac{d_{IN}}{d_{EX}}\right)^2\right]};$$

where MBΣ is maximum value of the total bending moment, Nm; WBis bend resistance moment, m3; dEX is external shaft diameter, m; dIN is internal shaft diameter, m; dIN / dEX = 0,8…0,95 relative dimension of the internal shaft diameter; Mtq is value of torque moment in the calculated cross section, Nm; PAX is axial force in the calculated cross-section, N; FC is area of the shaft calculated cross-section, m2.

To determine the equivalent stress σEq by the third theory of strength, MPa:

$$\sigma_{Eq} = \sqrt{\left(\sigma_T + \sigma_B\right)^2 + 4 \cdot \tau_{tq}^2}$$

To compare the operating equivalent stress in the dangerous shaft cross section with the allowable stress k0,2= σ0,2 / σEQ (σ0,2 is yield point of material under tension) after the execution of computations on strength. At the same time the safety margin must be equal to k0.2 t 1.5...2. Initial data for turbine shaft strength calculation:[7]
distance from the front support to a compressor rotor center of mass:

$$a = 65mm = 0.065 \text{ m} ;$$

distance from the rear support to a turbine rotor center of mass:
b = 125mm = 0.125 m ;
distance between supports:

$$Lbearing = 0.718 \text{ m} ;$$

torque transmitted through the turbine shaft:

$$M_{tq} = \frac{N_{hpt}}{\omega_{HPR}} =32528000/1224.994=26554$$

gyroscopic torque of high pressure compressor rotor:
MGc = Jpc·ωHPR·Ω =14.291*1224.994*0.265=4637.057
gyroscopic torque of high pressure turbine rotor:

$$M_{Gt} = J_{pt} \cdot \omega_{HPR} \cdot \Omega =3.38*1224.994*0.265== 1083.098 \cdot N \cdot m$$

centrifugal force of compressor rotor unbalanced weights:
RunbC = 0.225·kN;
centrifugal force of turbine rotor unbalanced weights:
RunbT = 0.225·kN;
compressor rotor mass:
MC = 103.784 kg ;
turbine rotor mass:
MT = 132.088 kg ;
turbine shaft external diameter:
dEX = 125·2mm = 0.25 m ;

turbine shaft axial force:

$$PAXT = -248.236 \cdot kN;$$

turbine shaft material yield strength:

$\sigma_{0.2} = 850MPa.$

Total transversal forces in vertical plane are:

for compressor shaft: $RcsC = 4.298 \cdot kN;$

for turbine shaft $RcsT = 5.408 \cdot kN.$

Reactions in supports caused by transversal forces are equal to:

$$R_{Ay} = \frac{R_{csC} \cdot (L_{bearing} - a) + R_{csT} \cdot b}{L_{bearing}} = 4.85 \cdot kN ;$$

$$R_{Bv} = \frac{R_{csC} \cdot a + R_{csT} \cdot (L_{bearing} - b)}{L_{bearing}} = 4.856 \cdot kN;$$

Reactions in supports caused by gyroscopic moments are:

$$R_{Az} = -\frac{M_{Gc} + M_{Gt}}{L_{bearing}} = -7.967 \cdot kN;$$

$$RBz = -RAz = 7.967 \cdot kN;$$

After constructing the diagram of forces and momenta from fig. 7 obtain the dangerous shaft section at the compressor center of mass, where

$Mb\Sigma = 671.56N \cdot m$

Turbine shaft internal diameter is dIN = shaft section area equals:

After constructing the diagram of forces and momenta from fig. 7 obtain the dangerous shaft section at the compressor center of mass, where $Mb\Sigma$ 671.56N m Turbine shaft internal diameter is dIN 123 2 mm 0.246m ; shaft section area equals:[9]

$$F_{sh} = \frac{\pi}{4} \cdot \left(d_{EX}^{2} - d_{IN}^{2}\right) =$$

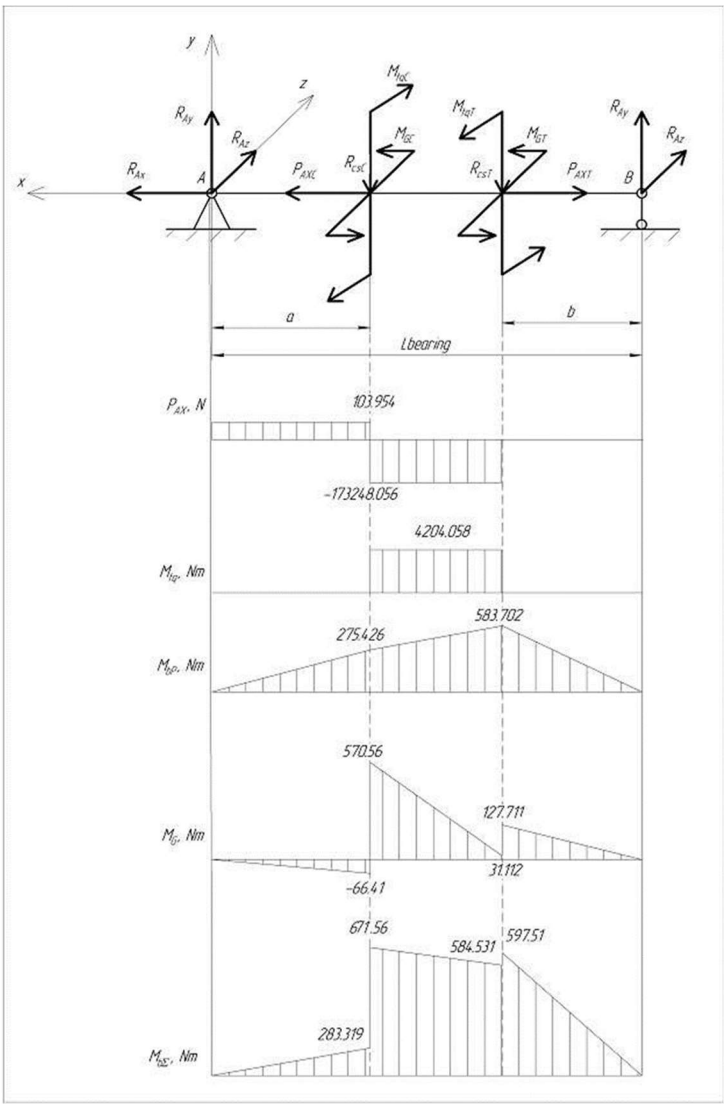

Figure 5. Diagram of forces and momenta acting on the high pressure rotor

Bending stress in shaft design section is equal to:

$$\sigma_{shb} = \frac{32 \cdot M_{b\Sigma}}{\pi \cdot d_{EX}^{3} \cdot \left[1 - \left(\frac{d_{IN}}{d_{EX}}\right)^{4}\right]} = 7 \cdot MPa$$

tensile stress in shaft design section is:

$$\sigma_{tens} = \frac{\left|P_{AXT}\right|}{F_{sh}} = 159.306 \cdot MPa$$

tangential stresses in shaft design section is:

$$\tau_{sh} = \frac{16 \cdot M_{tq}}{\pi \cdot d_{EX}^{3} \cdot \left[1 - \left(\frac{d_{IN}}{d_{EX}}\right)^{4}\right]} = 138.12 \cdot MPa$$

equivalent stress is determined according to the theory of the greatest tangential stresses, and is used as a criterion of shaft composite stressed state:

$$\sigma_{\Sigma eq} = \sqrt{\left(\sigma_{shb} + \sigma_{tens}\right)^2 + 4 \cdot \tau_{sh}^2} = 322.448 \cdot MPa;$$

Safety margin for the shaft in dangerous section is determined as

$$k_{0.2} = \frac{\sigma_{0.2}}{\sigma_{\Sigma eq}} = 2.636$$

3.2 Calculation of Ceramic Hybrid Bearings

The bearing calculation is necessary to execute in such sequence:

- calculation of geometry;
- calculation of magnetic chain;
- calculation of winding;[10]

Initial data for active magnetic bearing calculation:

diameter of the rotor:

d 250mm 0.25 m

air gap:

$g_{\backslash}$ 0.7mm;

maximum value of the magnetic induction:

Bmax= 1.4tesla;

maximum driving force:

Fmax=5kN;

factor of groove area filling with copper:

kCu= 0.5;

current in the system:

imax =100A;

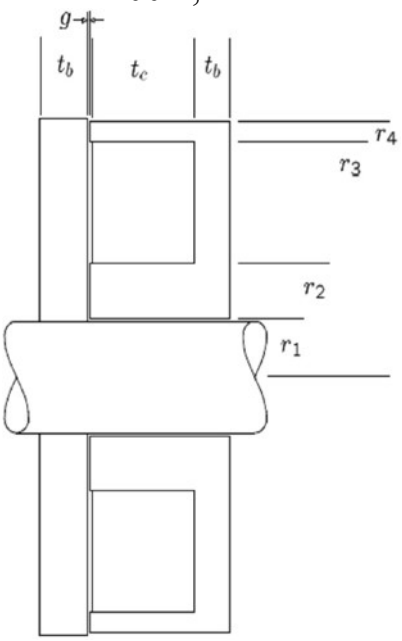

Figure 6. Axial bearing

$$r_1 = \frac{d}{2} + g =$$

0.126

Second radius equals:

$$r_2 = \sqrt{\frac{\mu_0 \cdot F_{max}}{\pi \cdot B_{max}^2} + r_1^2} =$$

0.13 m

Winding groove is:

$$t_c = \sqrt{\frac{2g \cdot B_{max}}{\mu_0 \cdot k_{Cu} \cdot j_{max}}} =$$

0.025

where, jmax is allowable current density and is equal to:

jmax= 2.636

jmax=509.295

All other parameters from figure 6 are equal to:

$$r_3 = r_2 + t_c =$$

0.155

$$r_4 = \sqrt{r_2^2 - r_1^2 + r_3^2} =$$

0.154

$$t_b = \frac{\left(r_2^2 - r_1^2\right)}{2r_2} =$$

0.003

Area occupied by the coil in the groove is equal to:

$$A = \pi\left(r_4^2 - r_3^2\right) =$$

0.003 m2

Sectional area of the conductor is:

$$a_0 = \frac{i_{max}}{j_{max}} =$$

19.435*10^-6

The number of windings is equal to:

$$n = \frac{k_{Cu} \cdot A}{a_0} =$$

81.632

Medium length of the winding is equal to:

$$l_m = \pi \cdot \left[d + 2g + 2 \cdot \left(r_2 - r_1\right) + t_c\right] =$$

0,893

Power of heat loss is equal to:

$$P = \frac{R \cdot i_{max}^{2}}{4} = 44.234$$

where, R is ohmic resistance and is equal to:

$$R = \frac{l_m \cdot n \cdot \rho}{a_0} = 0.067\ \Omega$$

CHAPTER 4:DEVELOPMENT OF THE ENGINE OIL SYSTEM AND ANALYSIS OF MEASURES FOR THE APPLICATION OF BEARINGS

4.2 Brief description of designed oil system

The oil system is divided into two types according to the oil usage method:
-Acyclic (disconnected, open loop) and
-Loop (closed loop).
In a non-circulating system, a lubricating liquid (oil or main fuel) is used at a time. Unload it from the engine after pumping it through the lubricating object (. Due to the limited number of units in the system, this type of oil system is very simple and lightweight. In this type of system, pressurized oil is usually used instead The pump oil is supplied to the lubrication object. The main drawback of the incoherent oil system is the large consumption of lubricating fluid. This is why they are used in GTEs that are one-time or short-term operation.

4.2 analysis of measures for the application of bearings

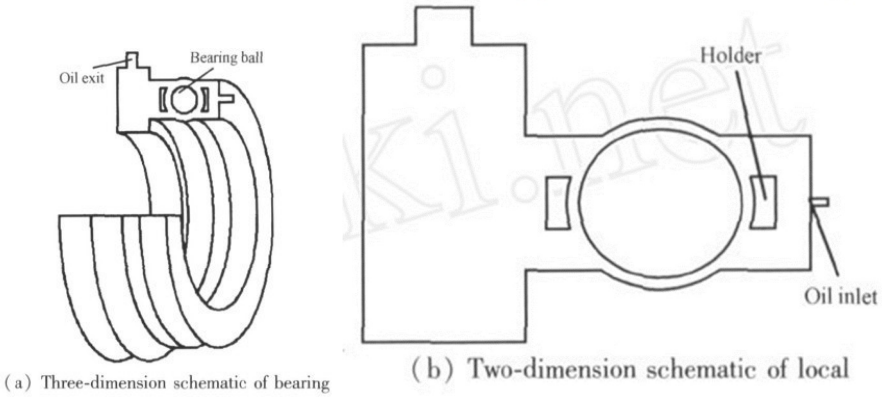

(a) Three-dimension schematic of bearing (b) Two-dimension schematic of local

The lubricating oil appears at the entrance. The reason is that when the lubricating oil is sprayed into the bearing cavity, due to the obstacles of the bearing to keep the frame, some oil flow occurs back. If the oil stays in the bearing cavity for too long, it will cause the bearing cavity to overheat; if the stay is too short, it may cause insufficient lubrication to form a certain area of oil flow, which will cause the "air rotation" phenomenon to exacerbate the bearings of the bearings Wear.
1) The fault of the bearing will cause the engine rotor to increase or even serious accidents, so the reliability of the bearing is required;
(2) Under the condition of high temperature to 315CO and low temperature to -250CO, the bearings can work normally and have a long service life;
(3) The bearing can withstand the radial load of the rotor, or at the same time, the radial and axial load at the same time, and have a large bearing capacity;
(4) Light structural weight and sufficient rigidity can ensure the transmission between rotating shafts to the bearing seat, and alleviate the impact and vibration between them;

4.3 Monitoring of Ceramic Hybrid Bearings failure in oil system

The monitoring of the bearing temperature generally close the temperature sensor close to the bearing outer ring. The temperature change of the bearing is a slow process. It is not sensitive to the slight failure of the bearing in the early days. Only when the bearings have occurred in a serious failure, the bearing temperature will change rapidly.

Vibration monitoring is divided into monitoring of the shaft system and the monitoring of the vibration acceleration of the body. The shaft vibration signal is the most direct signal that reflects the state of the axis and the failure. The bearing failure can immediately cause changes in the vibration state. The power consumption of the system is also an important parameter that reflects the state of the axis and the failure. When the test bearing fails or fails, it will inevitably cause the motor output power to increase.

4.4 The lubrication and cooling method of the bearings

Lubricate under the ring

Adapt to the needs of lubrication and cooling of high DN value bearing. The so -called underwriting lubrication is the radial hole and slot of the inner ring of the bearing of the bearing of the coating, that is, the oil from the bearing from the bottom ring of the bearing to the bearing, not like the ejection lubrication is sprayed directly into the bearings from the bearing end surface. The lubrication structure under the ring is basically composed of two parts, namely the oil collection department and the oil transfer department.

The characteristics of lubrication under the ring.

The prominent advantage is that the bearing temperature can be reduced, especially the working temperature of the inner circle is lower than the outer circle under various working conditions, which is more advantageous to the internal gap in the bearing, and can effectively prevent high -speed light loading under the inner ring. Broken injury failure. Secondly, due to the reasonable oil flow road, the utilization rate of oil oil is high. The spray lubrication can only be used for 70%oil oil, while the underwriting lubrication can reach more than 80%under the condition of reasonable structural design, up to 95%. At the same time, this structure greatly reduces the loss of mixing, reduces power loss, and reduces the chance of dirt in the oil in the oil. Adapt to the needs of lubrication and cooling of high DN value bearing.

Nozzle lubrication

This lubrication method is mainly used in the bearing lubrication of the shaft. Because the inner and outer ring of the bearing of the shaft cannot be installed at the same time, the nozzle cannot be installed, so the spray lubrication or under the ring lubrication cannot be implemented. In the case of no loop lubrication, you can also simultaneously aim at the lubricating oil in the oil pipe that is parallel to the axis.

Features of nozzle lubrication

The lubrication method, the oil flow is difficult, and the penetration power is extremely poor. Therefore, the bearing lubrication and cooling are generally not sufficient, and the surface often becomes black, or even the hardness decreases. This lubrication method should be paid special attention in design: first, to increase the spray flow of nozzles appropriately; second, the diameter of the oil pipe is increased, and the inner wall is smooth to ensure smooth oil circulation. Third, the bearing material should be high -temperature heat -resistant alloy Essence.

Aviation bearing disorders --- Through statistical analysis, the failure mode of the engine's spindle bearing is roughly divided into 15 categories

1 scratches, abrasions ; 2 wear ; 3 Light load slipping ; 4 rust ; 5 eccentric wear, load trajectory down ; 6 pressure pit, collision injury ; 7 fatigue spalling ; 8 current erosion ;

9 cage deformation ; 10 cracks ; 11 cage silver layer off ; 12 bipolar wear cat eye ; 13 heat discoloration ; 14 size expansion or reduction ; 15 vibration patterns.
The direct result of failure is temperature rise, increased vibration or vibration state changes, shaft power consumption increases, the axis trajectory shape changes

Fig diagram of the oil system of the engine

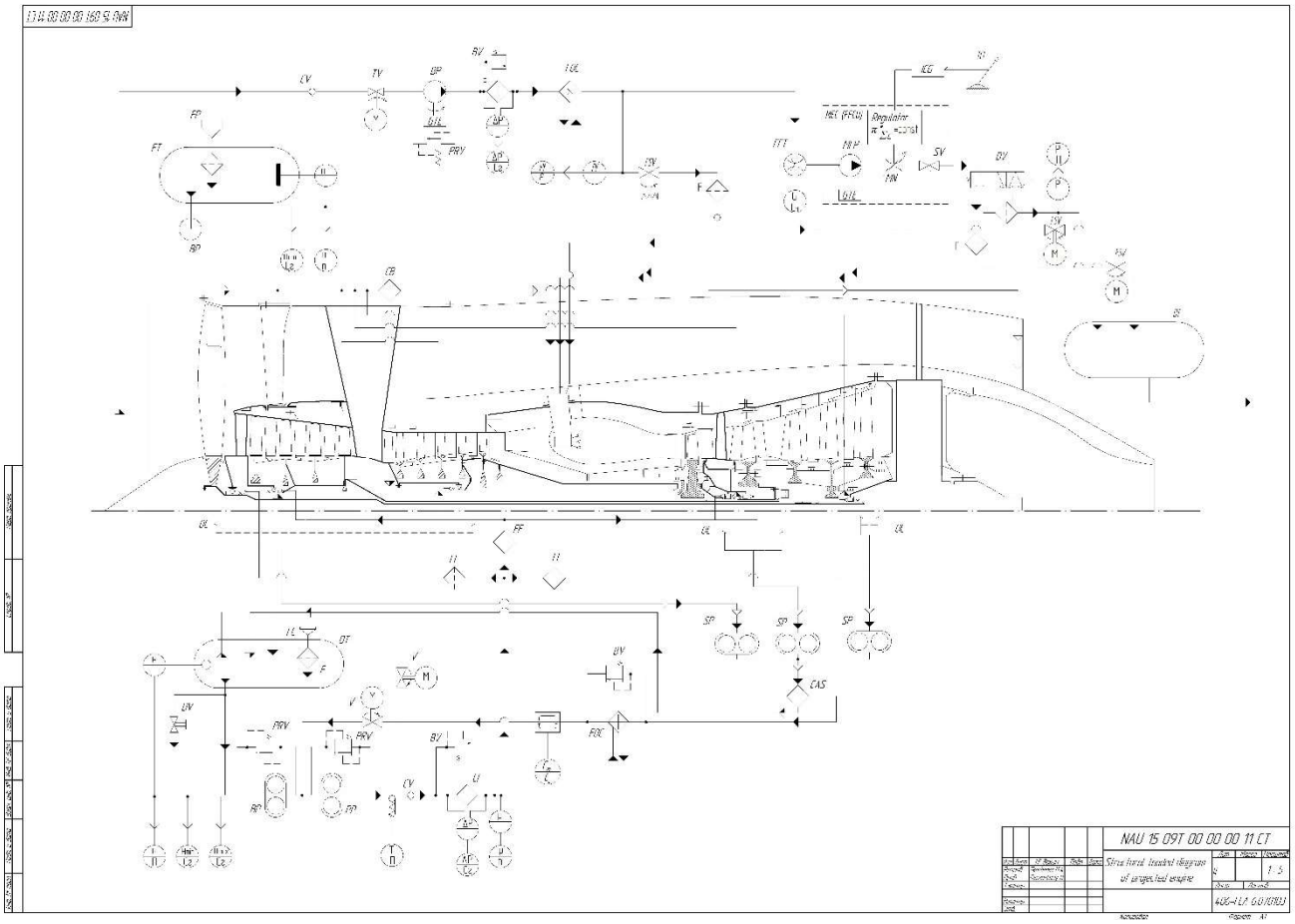

APPENDIX D

CHAPTER 5 LABOR PRECAUTION

Labour Protection (or Occupational Safety and Health)

This paper mainly discusses the occupational labor protection and safe working environment of ***high-altitude personnel in civil aviation maintenance.***

Falls from height are one of the biggest causes of workplace fatalities and major injuries. Common causes are falls from ladders and through fragile roofs. The purpose of WAHR is to prevent death and injury from a fall from height. Each year in the air transport and aviation industry, HSE receives reports of employees injuring themselves after failing from a height.

Falls from height can cause permanent and debilitating injuries. The risk of serious injury or death from a fall increases significantly when working at heights of more than two meters. This safety bulletin is issued to remind maintenance staff and the supervisors, that working at heights requires adequate fall from height risk controls.

Employers and those in control of any work at height activity must make sure work is properly planned, supervised and carried out by competent people. This includes using the right type of equipment for working at height. Low-risk, relatively straightforward tasks will require less effort when it comes to planning. Employers and those in control must first assess the risks. Take a sensible, pragmatic approach when considering precautions for work at height. Factors to weigh up include the height of the task; the duration and frequency; and the condition of the surface being worked on. There will also be certain low-risk situations where common sense tells you no particular precautions are necessary.

Labor protection is the general term for national and units to protect the safety and health of workers in the process of labor production. It refers to based on national laws and regulations, relying on technical progress and scientific management, adopting organizational measures and technical measures, eliminating adverse conditions and behaviors that endanger personal safety and health, prevent accidents and occupational diseases, and protect the safety and health of workers in the labor process.

Labor protection includes the safety requirements of the use, storage and disposal of flammable materials; the safety requirements of the use and disposal of toxic materials; the safety requirements for the protection of meteorological radar waves; the safety requirements of maintenance personnel listening and vision protection; the safety work procedure of high -altitude operation.

5.1 Harmful and hazardous working factors

Falls from height can cause permanent and debilitating injuries. The risk of serious injury or death from a fall increases significantly when working at heights of more than two meters. This safety bulletin is issued to remind maintenance staff and the supervisors, that working at heights requires adequate fall from height risk controls. Identifying hazards involves recognizing things that may cause injury or harm to the health of a person, such as where a person may fall from, through, or into a place or thing such as:

- Wet and uneven surfaces
- Faulty equipment (harness, fall protection gears)
- Weather conditions
- Insufficient training
- Improper footwear used
- Structures (the stability of temporary or permanent structures)
- Edges (edge protection for open edges of floors, working platforms)
- The proximity of workers to unsafe areas
- Movement of plant or equipment (ensuring there is no sudden acceleration or deceleration)

Working at height remains one of the biggest causes of fatalities and major injuries. Common cases include falls from roofs, ladders, and through fragile surfaces. 'Work at height' means work in any place where, if there were no precautions in place, a person could fall a distance liable to cause personal injury (for example a fall through a fragile roof down an unprotected lift shaft, stairwells).

5.2 Analysis of working conditions

It is the responsibility of every employer to ensure, to the extent reasonably practicable, that the access devices used by its employees and others are secure. Reasonably practicable but appropriate and effective measures shall be taken to prevent any personal injury from falling distances. Employers should first assess the risks. Factors to weigh up include the height of the task, the duration and frequency, and the condition of the surface being worked on.

Before working at height they should work through these simple steps:
avoid work at height where it's reasonably practicable to do so where work at height cannot be easily avoided, prevent falls using either an existing place of work that is already safe or the right type of equipment minimize the distance and consequences of a fall, by using the right type of equipment where the risk cannot be eliminated.
For each step, always consider measures that protect everyone at risk (collective protection) before measures that only protect the individual (personal protection)
Collective protection is equipment that does not require the person working at height to act for it to be effective. Examples are permanent or temporary guardrails, scissor lifts and tower scaffolds.
Personal protection is equipment that requires the individual to act for it to be effective. An example is putting on a safety harness correctly and connecting it, with an energy-absorbing lanyard, to a suitable anchor point.

The following are all requirements in law that you need to consider when planning and undertaking work at height. You must:
■■ take account of weather conditions that could compromise worker safety;
■■ check that the place (eg a roof) where work at height is to be undertaken is safe. Each place where people will work at height needs to be checked every time, before use;
■■ stop materials or objects from falling or, if it is not reasonably practicable to prevent objects falling, take suitable and sufficient measures to make sure no

one can be injured, eg use exclusion zones to keep people away or mesh on scaffold to stop materials such as bricks falling off;
■■ store materials and objects safely so they won't cause injury if they are disturbed or collapse;
■■ plan for emergencies and rescue, eg agree a set procedure for evacuation. Think about foreseeable situations and make sure employees know the emergency procedures. Don't just rely entirely on the emergency services for rescue in your plan.

5.3**development of protective measures**

One of the main problems with providing safe access to an aircraft without special docking is the need to follow the circular fuselage shape. Great attention to detail is required to ensure there are no visible and dangerous gaps between the aircraft and the work platform

1) When planning visits, the needs of all users should be considered to ensure compliance with regulatory requirements (Cooperation and Coordination).

2) Edge protection should be provided for any edge where personnel may fall for a certain distance, such as working platforms, towers, and scaffolding, which may easily cause personal injury. (Typically, the fuselage of an aircraft will provide edge protection for at least one edge).

3) Openings in the fuselage of the aircraft, such as doors and cargo compartments, shall be provided with edge protection, access in accordance with the criteria discussed in the remainder of this SIM, or remain closed. The straps provided to aircraft door frames are not fall protection and are not suitable as edge protection. However, a proprietary edge protection system for opening doors is available

4) Skirting should be installed on edges where objects such as tools and materials could fall and cause injury. Additional protection may be required if loose items are stacked at a height above the toe board, similar to the "brick guards" seen on construction sites. These measures also help prevent damage to the aircraft skin.

5) The clearance between the work platform and the aircraft may vary depending on the nature of the work being performed. However, it should always be as small as possible, and never so large that a person or object can fall. If this is not possible, edge protection should be provided, including toe boards if necessary.

6) When working from the skin of the aircraft itself, there should be measures to prevent or mitigate the fall, such as work by an operator standing on the wing

7) Access equipment such as scaffolding should be stable. Scaffolding will most likely not be assembled in an accepted standardised configuration, so there should be evidence that strength and stability calculations have been made.

8) The access to the scaffolding and deck is preferably inside, and the entrance of each platform should be fitted with trap doors. Channels should be strong enough to withstand the weight of any materials or equipment occupied by the route.

9) In some cases, it is foreseeable that in aircraft maintenance, scaffolding will be so complex that a competent person is required to prepare a plan for assembly, use and disassembly.

10) No matter how you enter, you need to consider the means of escape in case of emergency. In most cases, access routes will not allow the same escape speeds in the event of a fire as traditional emergency stairs. If inspectors have any doubts about the adequacy of means of escape, they may wish to review the employer's fire risk assessment. If one is unavailable, or if there is doubt about its adequacy, the inspector should contact the fire brigade as an obvious matter.

Dos and don'ts of working at height

Do…

- as much work as possible from the ground;
- work off scaffolding in preference to working off ladders
- ensure workers can get safely to and from where they work at height;
- ensure equipment is suitable, stable and strong enough for the job, maintained and checked regularly;
- take precautions when working on or near fragile surfaces;
- provide protection from falling objects;
- consider emergency evacuation and rescue procedures.

Don't…

- overload ladders – consider the equipment or materials workers are carrying before working at height. Check the pictogram or label on the ladder for information
- overreach on ladders or stepladders;
- rest a ladder against weak upper surfaces, e.g. glazing or plastic gutters;
- use ladders or stepladders for strenuous or heavy tasks, only use them for light work of short duration (for example a maximum of 30 minutes at a time);
- let anyone who is not competent (who doesn't have the skills, knowledge and experience to do the job) work at height.

5.4 **Types of access equipment**

A wide range of access equipment is used in the industry. This includes suspended work platforms specially built for aircraft refinishing work, decking that is customised to fit all or part of an aircraft, docking that can be adjusted in height and profile for a range of aircraft (eg nose and tail docking), various types of scaffolding, mobile elevating work platforms (MEWPs), towers and steps.

Special docking equipment (sometimes referred to as 'scene docks' or 'jigs') represents a substantial investment, but it can provide safe access as it can be adjusted to closely follow aircraft contours. Systems may be a part of the hangar structure and may be placed in a number of horizontal and vertical combinations.

More common are customised docking and scaffolds, which are usually permanent

mobile structures.
Work equipment, for example scaffolding, needs to be assembled or installed according to the manufacturer's instructions and in keeping with industry guidelines. Where the safety of the work equipment depends on how it has been installed or assembled, an employer should ensure it is not used until it has been inspected in that position by a competent person. A competent person is someone who has the necessary skills, experience and knowledge to manage health and safety. Any equipment exposed to conditions that may cause it to deteriorate, and result in a dangerous situation, should be inspected at suitable intervals appropriate to the environment and use. Do an inspection every time something happens that may affect the safety or stability of the equipment, eg adverse weather, accidental damage. You are required to keep a record of any inspection for types of work equipment including: guard rails, toe-boards, barriers or similar collective means of protection; working platforms (any platform used as a place of work or as a means of getting to and from work, eg a gangway) that are fixed (eg a scaffold around a building) or mobile (eg a mobile elevated working platform (MEWP) or scaffold tower); or a ladder. Any working platform used for construction work and from which a person could fall more than 2 metres must be inspected:
■■ after assembly in any position;
■■ after any event liable to have affected its stability;
■■ at intervals not exceeding seven days.
Where it is a mobile platform, a new inspection and report is not required every time it is moved to a new location on the same site. You must also ensure that before you use any equipment, such as a MEWP, which
has come from another business or rental company, it is accompanied by an indication (clear to everyone involved) when the last thorough examination has been carried out.

5.5 Fire Safety Rules at the workspace

The best insurance against an aircraft fire is professional maintenance and a thorough preflight inspection. Always look for evidence of fuel, oil, and hydraulic leaks, and use your nose as well as your eyes. Carefully check under the cowl for bird nests, windblown debris, and misplaced rags. Check the exhaust stacks for security and cracks, and look for loose or leaking fittings on the brakes. Before takeoff, test all the electrical components that you might use during flight, and watch for any indications of impending failure. A pitot heat switch that fails and burns is much easier to cope with on the ground than while you enter the clouds at 1,000 feet. Fortunately, aircraft fires are relatively rare, but considering the serious consequences, particularly in flight, it's important to know the procedures for dealing with a fire, and to practice them often. Get out that emergency checklist, and make sure you know exactly what to do when a fire heats up your flying.

Dealing with an in-flight fire is a difficult proposition, but without the right tools it can be virtually hopeless. Part of your preflight check should include the fire extinguisher. Don't just see that it's there, look at its gauge and make sure it's in the green. Commercial operators must service, inspect, and weigh aircraft fire extinguishers monthly, and Part 91 operators should adopt a similar routine. Several types of extinguishers are commonly used for fighting aircraft fires, and it's important

to distinguish between them. They have different characteristics, and some are better suited to particular situations than others.

5.6 **Conclusions**

Falls from height are one of the biggest causes of workplace fatalities and major injuries. Common causes are falls from ladders and through fragile roofs. Work at height means work in any place where, if there were no precautions in place Strict compliance with labor laws, guidelines, industry standards, rules and regulations aimed at protecting the health of workers is required. the main task of occupational safety is to create safe and healthy working conditions for employees, makes a great contribution to improving flight safety. This is one of the current problems of civil aviation., a person could fall a distance liable to cause personal injury.

6.1 Background information

Air transport connects the world, bringing people and goods together. But the benefits of aviation also have an environmental downside. Emissions, noise, industrial processes, and waste must be managed by the industry, reduced, and where possible eliminated. In addition, aviation has a role to play in tackling the global issue of wildlife trafficking. Airport operations are an important factor in our economy, for tourism, imports, exports and business. However, these benefits must be weighed against the impact air travel is having on the quality of life of increasing numbers of people and on the local and global environment. Noise and air pollution – both from aircraft and from airport ground operations – are a problem for those who live, work and study around airports.

6.2 Noise Pollution

The most immediate impact of aircraft is noise – whether it is the regular rumble of international jets or the buzz of microlights and light aircraft on sunny afternoons. The noise from airborne aircraft is related to air speed. Any fast-moving components, such as propellers and compressor blades, generate noise, as do the exhaust gases of jets. Aircraft are also responsible for an increasing proportion of air pollutant emissions, both at local and global level.

The International Civil Aviation Organisation (ICAO) is responsible for drawing up aviation noise standards with the European Civil Aviation Conference, and UK standards are set in accordance with these.

Measures introduced to reduce noise include Noise Preferential Routes and restrictions on night flying. Maximum noise limits for departing aircraft are set and monitored and noise insulation schemes are in operation. Noise from aircraft on the ground is the responsibility of the airport operator. To comply with the EU Environmental Noise Directive, operators of airports with over 50,000 movements a year have been required to draw up Noise Action Plans。

Noise limits have been introduced at the designated airports to cover the period 0700h – 2300h. Airport companies are responsible for monitoring compliance and breaches are subject to a financial penalty. Night flights are restricted between 2300h – 0600h and airports are given quotas of the number of night movements of noisier aircraft allowed to land during these periods.

6.3 air pollution

Aircraft engines generally combust fuel efficiently, and jet exhausts have very low smoke emissions. However, pollutant emissions from aircraft at ground level are increasing with aircraft movements. In addition, a large amount of air pollution around airports is also generated by surface traffic. The main pollutant of concern around airports is nitrogen dioxide (NO2). NO2 is formed by nitrogen oxide (NOx) emissions from surface traffic, aircraft and airport operations. PM2.5 is also of concern, since particulate emissions from jet exhausts are almost all in this fine fraction. NOx in the lower atmosphere contributes to the production of ozone; ozone in the lower atmosphere is a pollutant, and contributes to global warming. Nitrogen oxides from

high-altitude supersonic aircraft are thought to damage the stratospheric ozone layer, the protective layer that filters out harmful radiation from the sun.

6.4 Solution

the aircraft fleet is becoming progressively more efficient, with aero-engine fuel efficiency per tonne-km down around 10% over the last six years; there will be further improvements coming on-line continuously in the near future as airlines take delivery of more lean-burning aircraft and start to replace fossil fuels with sustainable fuel alternatives. While these improvements by themselves will not be enough to offset completely the effect of traffic growth, they are a major component in the process of the industry starting to make real change in controlling its emissions.

- Support the rapid transition to the wide-spread use of sustainable aviation fuels for long-haul flights in particular. SAF is too expensive and we must incentivise its production and use.
- Develop highly efficient, large-capacity, short-haul aircraft to handle passenger throughput.
- Undertake a total fleet renewal by 2050 so that aircraft only fly if they are wholly or partly electric, or for longhaul flights only use SAF.
- Bridge the gap to electrification of short-haul passenger aircraft through hybridisation and improving battery energy densities, while developing hydrogen fuel-cell and electrofuel technology and infrastructure.
- Change the European air traffic management network, and encourage environmental improvements through provision of shorter and better routes.

Under international law, aviation fuel for international flights is exempt from taxation, which means air travel is relatively cheap. This also reduces the incentive for airlines to invest in more efficient aircraft. Aircraft operators are included within the European Union Emissions Trading Scheme. They could be further incentivised via fuel tax (which could be levied for domestic flights). This could: ensure airlines pay for the pollution they cause, like other transport operators encourage the development of more fuel-efficient aircraft help reduce the demand for air travel as other options become more competitive be consistent with UK pledges to reduce greenhouse gas emissions from airport operations Policy should progressively seek an equitable cost/taxation basis across all modes of transport. In particular, all possible attempts should be made to ensure that the costs of aviation fully include the environmental and social costs, in accordance with the “polluter pays” principle. The Government should also acknowledge the fact that the tax free status of aviation fuel effectively acts as a subsidy for the aviation industry, and should therefore fully factor this into its economic analysis of the costs and impacts of the industry.

6.5 ICAO

With a view to minimize the adverse effects of international civil aviation on the global climate, ICAO formulates policies, develops and updates Standards and Recommended Practices (SARPs) on aircraft emissions, and conducts outreach activities. These activities are conducted by the Secretariat and the Committee on Aviation and Environmental Protection (CAEP). In pursuing its activities, ICAO also cooperates with other United Nations bodies and international organizations.

The ICAO Assembly at its 40th Session in 2019 adopted Resolution A40-18: Consolidated statement of continuing ICAO policies and practices related to environmental protection — Climate change. It reiterated the two global aspirational goals for the international aviation sector of 2% annual fuel efficiency improvement through 2050 and carbon neutral growth from 2020 onwards, as established at the 37th Assembly in 2010. achieve the global aspirational goals and to promote sustainable growth of international aviation, ICAO is pursuing a basket of measures including aircraft technology improvements, operational improvements, sustainable aviation fuels, and market-based measures (CORSIA)。

6.6 Airfield environmental protection

To prevent the aircraft from polluting the environment around the airport, reduce or eliminate harmful substances to enter the environment, protect the physical and mental health of passengers and residents, and measure the administrative, legal, economic, and scientific and technological measures adopted.

The noise generated by the engine (including take -off, flight, landing, and ground trial) during operation (including take -off, flight, landing, and ground trials) can cause fatigue damage of the aircraft structure, affect the normal work of the instrument equipment on the aircraft and the comfort of passengers, and to the airport and nearby areas. Public life and work cause interference, and even affect people's health. Therefore, the international civil aviation organizations and aircraft production countries have made noise appraisal methods and maximum accommodation of civil transport aircraft.

In the late 1950s, since the jet passenger aircraft was put into civil aviation transportation, the noise of the aircraft caused serious attention and strong dissatisfaction with the public near the airport. Governments and worldwide professional organizations have begun to study airfield noise problems. At the international conference held in London in 1966, the conclusion of "reducing the noise and interference caused by civil aircraft". In 1969, the International Civil Aviation Organization (ICAO) held a special meeting on the noise of aviation noise near the airport. In 1971, it officially passed a document entitled "Aircraft Noise Standard and Suggestion Measures". six. International Standardization Organization (ISO) has also formulated international standard documents such as the "Expressing Methods of Available Available Innoic Noise" (ISO/R507-1970), "Monitoring of the Noise of Aerial Aircraft" (ISO/R1761-1970).

The aircraft engine discharge includes fuels and fuels that are leaked by the turbine engine and the burning smoke and gas sprayed out of the engine after burning the engine. These substances cause pollution around the environment around the airport. The leakage fuel is leaked from the fuel jet pipe due to mechanical reasons or improper manipulation during the decline in normal flight to fall into the decline and fall. The way to prevent is that the aircraft management department is strictly inspected. For planes that cannot prevent leakage fuel, they will not be issued to the operation certificate. The burning smoke was caused by incomplete fuel burning. The amount of smoke is represented by the value of smoke. The International Civil Aviation Organization stipulates that the normal smoke burning value of aircraft engines is 83.6 (F∞) (F∞ is engine power). The value -burning value discharged by aircraft engines

should not be greater than the specified values, otherwise it is considered unqualified. The three harmful gases sprayed by aircraft engines, namely undeaded hydrogen hydrogen hydride compounds, carbon monoxide, and nitric oxide, are expressed by grams, and there is a general measurement method internationally. The allowable content is dependent on the ratio of any gaseous pollutant mass DP to the engine power F∞ in the take -off and landing procedures. There are differences between the permission content of Asian speed flight and supersonic flight.

6.7 Support environmental protection at the economy level

Under international law, aviation fuel for international flights is exempt from taxation, which means air travel is relatively cheap. This also reduces the incentive for airlines to invest in more efficient aircraft. Aircraft operators are included within the European Union Emissions Trading Scheme. They could be further incentivised via fuel tax (which could be levied for domestic flights). This could:

- ensure airlines pay for the pollution they cause, like other transport operators
- encourage the development of more fuel-efficient aircraft
- help reduce the demand for air travel as other options become more competitive
- be consistent with UK pledges to reduce greenhouse gas emissions from airport operations

Policy should progressively seek an equitable cost/taxation basis across all modes of transport. In particular, all possible attempts should be made to ensure that the costs of aviation fully include the environmental and social costs, in accordance with the "polluter pays" principle.

The Government should also acknowledge the fact that the tax free status of aviation fuel effectively acts as a subsidy for the aviation industry, and should therefore fully factor this into its economic analysis of the costs and impacts of the industry.

Conclusion

Establish institutions and associations for the Aviation Environmental Protection Commission. Based on market rules and control policies. Formulate charging standards for aircraft abandoned emissions. The environmental benefits of the aviation system block upgraded, using more sustainable fuel.

References

1.MRC hybrid ceramic bearings for wind turbine generators/skf.com | skf.com/us/products/mrc/hybrid-ceramic-ball-bearings/PUB M880-610 · February 2020 · 20018-Id02G
2. SKF USA Inc Lansdale, PA 19446, USA ©2002 SKF (PDF ONLY 6/2011) Version 6/2011 Publication M880-600 Assessment. bit. J. High Technology Ceramics. 1985; 1(69).
3. Boca Bearings Engineering Guide /© Copyright 2004 - 2022 Boca Bearings, Inc. - All Rights Reserved
4. Manufacturing Engineering Society International Conference 2017, MESIC 2017, 28-30 June 2017, Vigo (Pontevedra),
5. Burrier HI. Optimizing the Structure and Properties of Silicon Nitride for Rolling Contact Bearing Performance. Tribology Transactions. Taylor & Francis Group ; January 1996; 39(2): 276–285.
6. Shaft and Bearing Calculations/Gert Hallgren ITT Flygt AB
applications: a review. Journal of Materials Education. 1995; 17: 245–303.
7. Raga R., Khader I., Zdeněk C., Kailer A. Experimental and numerical investigation of crack initiation and
propagation in silicon nitride ceramic under rolling and cyclic contact. Journal of Physics: Conference
Series. IOP Publishing; May 2017; 843(1): 12030. Available at: DOI:10.1088/1742-6596/843/1/012030
8. Nandi S., Toliyat HA., Li X. Condition Monitoring and Fault Diagnosis of Electrical Motors—A Review.
IEEE Transactions on Energy Conversion. December 2005; 20(4): 719–729.
9. Benbouzid ME., Vieira M., Theys C. Induction motors' faults detection and localization using stator current
advanced signal processing techniques. IEEE Transactions on Power Electronics. 1999; 14(1): 14–22.
10. Elbouchikhi E., Choqueuse V., Benbouzid M. Condition monitoring of induction motors based on stator
currents demodulation. International Review of Electrical Engineering. Praise Worthy Prize; 31 December
2015; 10(6): 704–715. Available at: DOI:10.15866/iree.v10i6.7594